SULFUR RECIRCULATION AND IMPROVED MATERIAL SELECTION FOR HIGH TEMPERATURE CORROSION ABATEMENT

KME-714

KME
CONSORTIUM MATERIALS TECHNOLOGY
for thermal energy processes

Sulfur recirculation and improved material selection for high temperature corrosion abatement

Investigating different aspects of corrosion memory

KRISTIAN VINTER DAHL
MELANIE MONTGOMERY
YOHANES CHEKOL MALADE
FLEMMING GRUMSEN
SØREN AAKJÆ JENSEN
LARS MIKKELSEN
OVE HAURIS JESPERSEN
NIELS PEDER HANSEN
SVEN ANDERSSON
MARIA DOLORES PAZ
TORBJÖRN JONSSON
JULIEN PHOTHER-SIMON
JESPER LISKE

ISBN 978-91-7673-093-5 | © 2018 Energiforsk

Energiforsk AB | Phone: 08-677 25 30 | E-mail: kontakt@energiforsk.se | www.energiforsk.se

Preface

The project has been performed within the framework of the materials technology research programme KME, Consortium materials technology for thermal energy processes, period 2014-2018. The consortium is at the forefront of developing material technology to create maximum efficiency for energy conversion of renewable fuels and waste. KME has its sights firmly set on continuing to raise the efficiency of long-term sustainable energy as well as ensuring international industrial competitiveness.

KME was established 1997 and is a multi-cliental group of companies over the entire value chain, including stakeholders from the material producers, manufacturers of systems and components for energy conversion and energy industry (utilities), that are interested in materials technology research. In the current programme stage, eight industrial companies and 14 energy companies participate in the consortium. The consortium is managed by Energiforsk.

The programme shall contribute to increasing knowledge within materials technology and process technology development to forward the development of thermal energy processes for efficient utilisation of renewable fuels and waste in power and heat production. The KME goals are to bring about cost-effective materials solutions for improved fuel flexibility, improved operating flexibility, increased availability and power production with low environmental impact.

KME's activities are characterised by long term industry and demand driven research and constitutes an important part of the effort to promote the development of new energy technology with the aim to create value and an economic, environmentally friendly and long term sustainable energy society.

The industry has participated in the project through own investment (60 %) and the Swedish Energy Agency has financed the academic partners (40 %).

Bertil Wahlund, Energiforsk

Abstract

The aim of the project was to study the Sulfur Recirculation technique as a possible solution to decrease the corrosion rates in waste fired CHP plants as well as the corrosion memory effect (both environment and material). The results show that the Sulfur Recirculation technique decreases the corrosion of the superheaters through a change in chemistry of the flue gas and formed deposits. The investigations also show that there is a corrosion memory effect (both environment and material), i.e. previous deposit build-up/oxide scale formation/alloy microstructure will influence the present corrosion attack. The environmental memory effect may influence the corrosion rate in two ways. An initially less corrosive deposit may reduce corrosion in a more corrosive environment while a corrosive deposit may increase corrosion in a less corrosive environment. The corrosion memory effect shows that an aged microstructure is more vulnerable for Cl induced corrosion.

Sammanfattning

Bränslevalet har stor inverkan på driften av en kraftvärmeanläggning. Biomassa och avfallsbränslen är normalt mer korrosiva än fossila bränslen vilket resulterar i lägre elverkningsgrad från dessa processer. Elproduktionen från pannor som förbränner biomassa och avfall är därigenom direkt beroende av effektivare korrosionsbegränsande strategier. I detta projekt har olika strategier att minska/kontrollera korrosionen undersökts:

- Svavelrecirkulationstekniken undersökts som en möjlig lösning för att minska korrosionshastigheterna i avfallseldade kraftverk.
- Hur mycket av den nuvarande korrosionen beror på korrosionshistoriken, dvs redan bildad beläggning, oxidskikt och material i stället för den aktuella rökgassammansättningen.

Effekten av svavelrecirkulationstekniken har studerats vid den första fullskaliga installationen i en kommersiell kraftvärmepanna. Resultaten ligger väl i linje med de preliminära indikationerna, dvs Svavelrecirkulationstekniken minskar korrosionen på överhettarna genom en förändrad rökgassammansättning och beläggningskemi.

Bränslemixen för kraftvärmeanläggning ändras normalt över tid, dvs det finns ett behov av att optimera och korrelera hur pannan körs till aktuell bränslekvalitet. En potentiell begränsningsfaktor för detta körsätt är perioder av accelererad korrosion, som sänker livslängden för t.ex. överhettare i pannan. Svavelrecirkulationsinstallation har i detta projekt använts för att undersöka hur korrosiviteten varierar över tid med variationer i bränslemixen. Hur mycket av den nuvarande korrosionen beror på korrosionshistoriken, dvs redan bildad beläggning och oxidskikt, i stället för den aktuella rökgassammansättningen, dvs den aktuella bränsleblandningen? Den första fullskaliga installationen av Svavelrecirkulation har i detta arbete fungerat som plattform för att studera korrosionsminneseffekten – miljö i och med möjlighet att använda två parallella linjerna vilka kan representera olika korrosiva bränslen. Resultaten visar att korrosionsminneffekten - miljö kan påverka korrosionshastigheten på två sätt. En mindre korrosiv beläggning kan minska korrosionen i en mer korrosiv rökgas medan en korrosiv beläggning kan öka korrosionen i en mindre korrosiv rökgas.

Den andra undersökta aspekten av korrosionsminnet är relaterad till bulkmaterialet. Hur kommer långsiktiga förändringar i legeringens mikrostruktur och samansättning påverka högtemperaturkorrosionsbeständighet? Korrosionsminneseffekten kan följaktligen uppdelas i två aspekter, dvs miljö och material. Materialaspekten har i projektet studerats genom både laboratorieundersökningar samt genom prover från olika anläggningar. Laboratorieundersökningen visade att stål med samma sammansättning blev mer sårbart för korrosion om det bildats Cr-rika inneslutningar. Korrosionsattacken observerades vid den Cr rika sigma-fas i KCl-rika miljöer. Dessutom uppvisade det från ett kraftverk åldrade 347H FG en snabbare korrosionshastighet än ett oexponerade stålet. Cr-rika inneslutningar observerades vid korrosionsfronten i

austenitiska stål exponerade i anläggningar i olika förbränningsmiljöer, dvs kol, rena träpellets + olja, rena träpellets + kol. Dessa Cr-rika inneslutningar identifierades till $M_{23}C_6$ i ett av de undersökta fallen

De erhållna resultaten kan bidra till att förstå hur processen i kraftverk med avancerade ångdata kan optimeras med avseende på variationer i bränslekvaliten. Genom att skapa långvarig kunskap om Svavelrecirkulationen och ta itu med korrosionsminneeffekten - miljön, kan pannans operatörer få verktyg för att minimera korrosionen med hjälp av smarta operativa strategier. Kunskapen om långsiktiga förändringar i mikrostruktur och sammansättning av legeringar påverkar dess högtemperatur korrosionsbeständighet kan dessutom hjälpa materialval och livstidspredikteringar av rostfritt stål i dessa pannor.

Måluppfyllelse

Det övergripande målet med projektet är att förbättra potentialen vid förbränning av biomassa/avfall. Detta har uppnåtts genom forskning vid en fullskalig installation av en ny korrosionsbegränsningsteknik som kallas svavelcirkulation samt genom att studera korrosionsminneseffekter. Projektets mål var att visa hur överhettarnas korrosionsangrepp förändras när svavelåtercirkulationstekniken körs under längre tid. Syftet var dessutom att skapa ny kunskap om två aspekter av korrosionsminne. Dessa uppgifter har genomförts framgångsrikt och projektkunskapen kan leda till förbättrad växtekonomi genom att:

- Ökad bränsleflexibilitet
- Ökad ångdata
- Bättre materialval för att förbättra långsiktig korrosionsbeständighet

Dessutom har projektet använt ett unikt förhållningssätt vid korrosionstestning. För att undersöka långsiktigt beteende hos utvalda överhettarmaterial, utfördes välkontrollerade förbehandlingar före exponeringarna. Därmed gavs en unik möjlighet att förutse långtidsbeteendet i olika typer av miljöer. En mer genomgripande måluppfyllelse presenteras senare i rapporten.

Nyckelord: Högtemperaturkorrosion, avfallseldade pannor, Svavelrecirkulationen, korrosionsminneseffekt-miljö, korrosionsminneseffekt-material

Summary

The fuel selection has a large impact on the operation of a Combined Heat and Power (CHP) plant. Biomass and waste fuels are normally more corrosive that fossil fuels resulting in lower electrical efficiency from these processes. The green electricity production from these boilers are thereby directly dependent on more effective corrosion mitigation techniques. The corrosion rate is influenced not only by the environment and materials used, but also by the history of the environment and materials, i.e. the corrosion memory. In this project, has two different strategies to control/limit the corrosion been investigated.

- Sulfur Recirculation technique has been investigated as a possible solution to decrease the corrosion rates in waste fired CHP plants by changing the environment.
- Investigating how the corrosiveness varies over time with variations in the fuel mixes. How much of the current corrosion attack is due to the corrosion environment history (i.e. previous deposit build-up and oxide scale formation) rather than the current flue gas composition (i.e. current fuel mix being used)?

The impact of the Sulfur Recirculation technique has been studied at the first full scale commercial installation in a commercial CHP boiler. The results are well in line with the preliminary indications, i.e. the Sulfur Recirculation technique decreases the corrosion of the superheaters through a change in flue gas composition and chemistry of the formed deposits.

The fuel selection for the CHP plants does normally change over time, i.e. there is a need to optimize and correlate the boiler operation to current fuel quality. A potential limiting factor in this type of operation is periods of accelerated corrosion, severely decreasing the lifetime of e.g. the superheaters in the boiler. The Sulfur Recirculation installation has in this project been used in order to investigate how the corrosiveness varies over time with variations in the fuel mixes. How much of the current corrosion attack is due to the corrosion environment history (i.e. previous deposit build-up and oxide scale formation) rather than the current flue gas composition (i.e. current fuel mix being used)? The first commercial full-scale installation has in this work provided an excellent platform in order to study the environmental corrosion memory effect with the two parallel lines representing different corrosive fuel. The results show that the corrosion memory effect – environment may influence the corrosion rate in two ways. An initially less corrosive deposit may reduce corrosion in a more corrosive environment while a corrosive deposit may increase corrosion in a less corrosive environment.

The other investigated aspect of corrosion memory is related to the bulk material. How will long-term changes in alloy microstructure and composition influence the high temperature corrosion resistance of the alloy? The corrosion memory effect can thus be divided into two aspects, i.e. environment and material. This was in the project studied both in laboratory investigations and through field samples. From

laboratory experiments it was shown that steels of the same composition behaved differently due to the presence of Cr rich precipitates. A preferential attack of Cr rich sigma phase in KCl bearing environments has been shown for the modified heat treated 310 steel, compared to the as received. In addition, aged 347H FG from a power plant had a faster corrosion rate than the as received steel (not aged microstructure). Cr rich precipitates were revealed at the corrosion front for lean austenitic steels exposed in the plant in different combustion environments, i.e. coal, clean wood pellets + oil, clean wood pellets + coal-fly ash. These Cr rich precipitates were identified in one case to be $M_{23}C_6$.

The obtained results may contribute to the understanding of how a power plant with advanced steam data can be operated with variations in fuel quality. By generating long term knowledge about the Sulfur Recirculation and addressing the corrosion memory effect - environment, boiler operators may benefit by getting tools to minimize the corrosion using smart operational strategies. The knowledge regarding long term changes in microstructure and composition of an alloys influence on its high temperature corrosion resistance may in addition aid material selection and lifetime predictions of stainless steels in these boilers.

Goal fulfilment

The overall goal of the project was to investigate strategies to improve plant economy and to increase the green electricity production. This has been achieved through research in a full-scale installation of a novel corrosion mitigation technique called Sulfur Recirculation as well as demonstrating the corrosion memory effect.

The project aim was to show how the corrosion attack of the superheaters is altered when the Sulfur Recirculation technique is activated. The aim was in addition to generate new knowledge of two aspects of corrosion memory. These tasks have been carried out successfully and the project knowledge may lead to improved plant economy by:

- Increased fuel flexibility
- Increased steam data
- Better material selection in order to improved long term corrosion resistance

Furthermore, the project has deployed a unique approach in corrosion testing. In order to investigate the long-term behaviour of selected superheater materials, well-controlled pre- treatments were performed to samples prior to the exposures. Thus, linking environment to the development of the different alloys gave a unique possibility to predict the long-time behaviour in different types of environment. A more thorough goal fulfilment is presented in the report.

Key words: High temperature corrosion, Sulfur Recirculation, corrosion memory-environment, corrosion memory-material

List of content

1 Introduction

1.1 BACKGROUND

The selection of fuel has a great impact on the total budget of a CHP plant. By choosing less expensive fuels (like different fractions of biomass or waste) the profit of the plant can increase greatly. Cheaper fuels are however usually more corrosive and the profit is decreased by increased maintenance costs, due to corrosion. In order to keep these costs low, the steam parameters are lowered, resulting in not only lower corrosion rates but also a drop in electrical efficiency. Hence, in order to increase the green electricity production from these corrosive fuels, more effective corrosion mitigation techniques are needed. This project aims to study the influence of one such technique, namely the Sulfur Recirculation technique. The corrosiveness of specific fuel types has been studied rather extensively and the boiler manufacturers use different boiler designs for different fuel mixes. However, little is known about how the corrosiveness varies over time with variations in the fuel mix. How much of the current corrosion attack is due to the corrosion history (i.e. previous deposit build-up and oxide scale formation) rather than the current flue gas composition (i.e. current fuel mix being used)? This effect can be referred to as a "corrosion memory". Another aspect of corrosion memory is related to the bulk material. How will long term changes in alloy microstructure and composition influence the high temperature corrosion resistance? The corrosion memory effect can thus be divided into two aspects, i.e. environment and material.

1.2 DESCRIPTION OF THE RESEARCH FIELD

1.2.1 The Sulfur Recirculation techniqe

The Sulfur Recirculation technique has previously been tested and evaluated for short term operation in a waste fired boiler [1]. The purpose of the Sulfur Recirculation technique is to reduce the corrosion rate of the superheaters in waste to energy plants by recirculating sulfur from the wet flue gas cleaning back to the boiler. The recirculated sulfur will increase the gas concentration of SO_2 in the boiler and decrease the Cl/S ratio of the deposits and ashes, thus producing a less corrosive environment for the superheaters [2, 3]. The innovative, patented Sulfur Recirculation process, for which Babcock & Wilcox Vølund AB (previously Götaverken Miljö AB) has a world-wide exclusive license, was invented by Hans Hunsinger at Karlsruhe Institute of Technology (KIT). The proposed technology is unique in the way that it, contrary to other methods, only uses the existing sulfur in the fuel and does not increase the amount of residues produced. The Sulfur Recirculation technique has previously been tested for shorter time spans (up to 1000 hours) at the Renova Waste-to- Energy facility in Göteborg. Corrosion probe measurements showed that corrosion rates were reduced by 50% or more (**Figure 1**) [1]

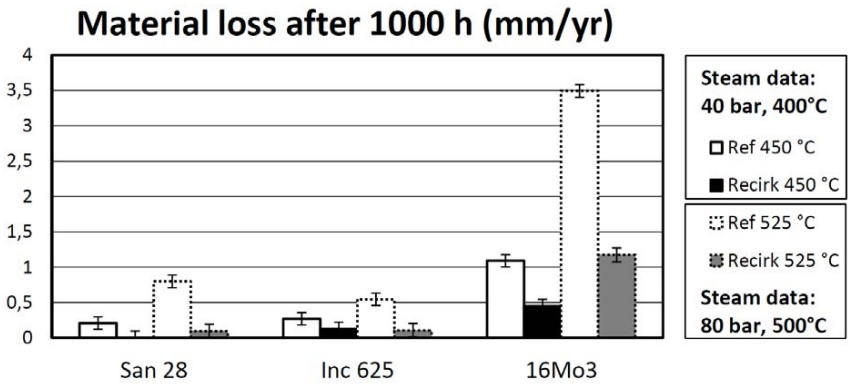

Figure 1. Corrosion rate in mm/year calculated from 1000 h exposures for 16Mo3, Sanicro 28 and Inconel 625 exposed at 450 and 525°C [1].

The corrosion probe tests performed at two different material temperatures showed that Sulfur Recirculation lowered the corrosion rates even when the material temperature was raised from 450 °C to 525 °C.

1.2.2 Corrosion memory - environment

The beneficial effect of sulfur addition on high temperature corrosion is well documented, see below. However, in contrast to other corrosion mitigation techniques based on sulfur containing species, the Sulfur Recirculation avoids the disadvantages of additional residue production. In fact, the residual fractions (e.g. sulphate water from the desulfurization part in the flue gas cleaning step) can be decreased by applying the Sulfur Recirculation technique. The Sulfur Recirculation aims to change the environment at the superheaters in order to limit the high-temperature corrosion. This is primarily done by decreasing the presence of alkali chlorides. The issue of alkali chloride induced corrosion has been previously studied and different ways to mitigate its effect have been addressed in recent years. A successful way to minimize the corrosiveness of alkali chlorides is to sulfate them to corresponding alkali sulfates. This can be done by using elemental sulfur, sulfur-rich additives or by co- combustion with a suitable fuel, e.g. sludge and coal [4-10]. The presence of sulfur in the fuel changes the flue gas chemistry; alkali chlorides react with SO_2/SO_3 forming alkali sulfates, and chlorine is released as HCl. There are several papers that investigate the gas phase reactions between alkali chlorides and sulfur containing species [7]. In addition to these publications, an investigation of the sulfation of solid alkali chlorides (i.e. deposits) and how they affect the corrosion has recently been published [8].

1.2.3 Corrosion memory – materials

The term memory effect for the material is related to the microstructural changes of bulk material that occur with exposure time at elevated temperature. Fujikawa et al. [11] investigated high temperature NaCl induced corrosion of austentic stainless steels and found that the depth of internal corrosion increased with C-content due to interaction between the corrosion and Cr-rich carbides. When the steels were first

aged at 650 °C to further precipitate carbides and then exposed to NaCl, the corrosion response was worsened. In effect this means that materials with good (short-term) performance in as delivered condition will perform worse with time/ temperature as a result of microstructure changes (memory effect). Experiences with biomass (KCl) induced corrosion from Danish plants strongly indicate that similar mechanisms could play a significant role.

Experiences from research and plant exposures including cooled probes, test superheaters and test tubes in existing superheaters [12, 13] have led to the choice of 18% Cr steels as the most suitable material for superheaters in biomass fired units. Exposure of steels and nickel based alloys with varying Cr contents indicate that there is a minimum in the chlorine induced corrosion attack around 15-18% Cr. With lower Cr content the alloys exhibit a high material loss while alloys with higher Cr contents are characterized by severe internal corrosion and chromium depletion [14, 15]. The measured corrosion rates are presented in Figure 2

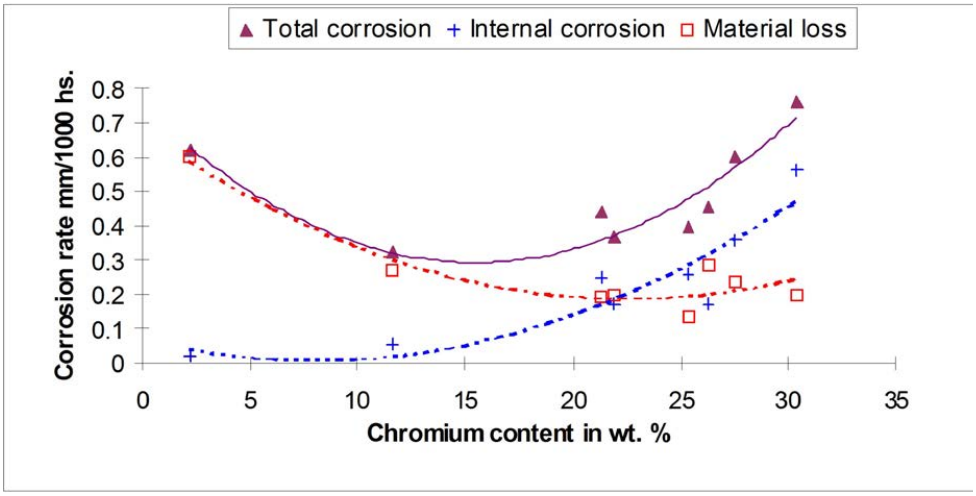

Figure 2. Effect of chromium content on corrosion rate, data from water-cooled probes in the superheater of a straw-fired CHP plant [14] . Flue gas temperature 700-800°C; metal temperature (average) 510-527°C; metal temperatures from 450-600°C were measured; exposure time was 1392 h.

Of particular interest for the present project is the increase in internal corrosion with the increase of Cr content. The mechanism behind this increase is not fully understood. Interestingly, the minimum in corrosion lies at the solubility limit of Cr in the steels (i.e. at higher Cr-contents Cr-rich precipitates will form), which makes it of high interest to study the influence of Cr-rich precipitates on the selective corrosion. It was hypothesized that the increase is coupled to the volatility of chromium chloride and that there might be a relation to the presence of Cr carbides [14]. Unfortunately no characterization of the bulk microstructure was done for the investigated alloys and therefore it is difficult to ascertain whether there were differences in carbide or other precipitate types, which are related to the Cr-content. Thermodynamic equilibrium calculations can help elucidate, whether such effects could be expected. Table 1 shows the Cr-content, the selective/internal corrosion rates and calculated phase fractions. From the data it can be seen that selective corrosion as a general trend follows the Cr-content but there are discrepancies, such as the poor performance of the Fe36Ni38Cr21 alloy. Remarkably the three alloys with the highest observed selective corrosion attack all have the tendency to form

the very Cr-rich bcc α-Cr (Calculated composition given in wt% for alloy Fe28Ni40Cr30: Cr 92.0, Mo 0.9, Fe 6.9, Ni 0.2).

	Cr wt%	Cr at%	Selective corrosion rate mm/1000h	FCC	ALFA-Cr	SIGMA	P_PHASE	NBNI3	NI3TI	M23C6	TiC
Fe28Ni40Cr30	30.3	32.5	0.58	0.802	0.188	-	0.004	-	-	0.006	-
Fe37Ni30Cr28	27.5	29.7	0.37	0.675	0.082	0.238	-	-	-	0.004	-
Fe36Ni38Cr21	21.3	22.8	0.26	0.808	0.064	0.098	-	-	0.026	-	0.003
Fe53Ni20Cr26	25.4	26.9	0.26	0.677	-	0.307	-	-	-	0.015	-
Fe3Ni63Cr22	21.9	24.9	0.18	0.695	-	-	0.199	0.080	0.004	0.022	-
Fe53Ni20Cr26	26.3	27.9	0.18	0.616	-	0.352	-	0.013	-	0.020	-
X20CrMoV121	11.6		0.05								
10CrMo910	2.2		0.02								

Table 1. Results of thermodynamic equilibrium calculations at 550°C for the alloys tested in [14]

1.3 RESEARCH TASK

In this current project, we aim to study the corrosion behaviour of superheaters during the first permanent full-scale installation of the corrosion mitigation technique "Sulfur Recirculation" and investigate if the reported short term positive effects on high temperature corrosion persist over time and simultaneously investigating the phenomenon corrosion memory - environment.

The present project also aims to look further into the role of the bulk microstructure on response to the chlorine-induced corrosion seen during biomass firing. It is hypothesized that an approach using a combination of modeling and controlled laboratory exposures can help elucidate the mechanism lying behind the increased selective corrosion seen for high Cr containing alloys.

1.4 GOAL

The overall goal of the project is to improve plant economy and to increase the green electricity production. This should be achieved through research in a full-scale installation of a novel corrosion mitigation technique called Sulfur Recirculation.

The aim is to show how the corrosion attack of the superheaters is altered when the Sulfur Recirculation technique is activated. The aim is in addition to generate new knowledge in order to better select materials for the superheaters. By demonstrating the success of these two aspects of corrosion memory this project may lead to improved plant economy by:

- Increased fuel flexibility
- Increased steam data
- Better material selection in order to improved long term corrosion resistance

Furthermore, the project will deploy a unique approach in corrosion testing. In order to investigate the long-term behaviour of selected superheater materials, well-controlled pre- treatments will be performed to samples prior to the exposures. Thus, linking environment to the development of the different alloys gives a unique possibility to predict the long-time behaviour in different types of environment.

1.5 PROJECT ORGANISATION

The project is jointly performed by Babcock & Wilcox Vølund AB, Babcock & Wilcox VølundA/S, Ørsted Bioenergy & Thermal Power A/S, Energy and Danish Technical University, MEC, Måbjergværket and HTC at Chalmers University of Technology, within the framework of KME. The distribution of work was:

Part	**Participants**	**Participants role in the project**
Babcock & Wilcox Vølund AB	Sven Andersson	Responsible for installation of the Sulfur Recirculation process. Evaluation of operation and corrosion.
Babcock & Wilcox Vølund A/S	Lars Mikkelsen	Responsible for corrosion probe test ports, superheater test material exposures and thickness measurements.
Ørsted Bioenergy & Thermal Power A/S Energy and Danish Technical University	Søren Aakjæ Jensen Kristian Vinter Dahl Melanie Montgomery Yohanes Chekol Malade Flemming Grumsen	Ørsted Bioenergy & Thermal Power A/S is funding DTU, which is responsible for developing and producing aged material as well as characterizing materials exposed in field and lab exposures.
MEC, Måbjergværket	Ove Hauris Jespersen Niels Peder Hansen	Plant operation.
Chalmers/HTC	Torbjörn Jonsson Maria Dolores Paz Julien Phother-Simon Jesper Liske	Project leader. Responsible for probe exposures and corrosion evaluation (both probe and coil tests).

Within the project the following researchers has been active: S. Andersson, L.Paz, J. Phother-Simon (Ph. D. Student), T. Jonsson, Y. Chekol (Ph. D. Student), K-V Dahl, M. Montgomery and J .Liske.

The industrial partners that have participated in the project are listed in the table below together with the amount of cash or in kind they have contributed with.

	Cash contribution	**In-kind contribution**	
Götaverken Miljö AB		1 927 kSEK	
B&W Völund		300 kSEK	
Dong Energy		1 663 kDKK*	
Dong Energy, Måbjergværket		300 kSEK	
Energy companies through Elforsk	76 kSEK		
Total industrial contribution	**76 kSEK**	**4 548 kSEK**	**= 4 624 kSEK**
STEM financing	**51 kSEK**	**3 032 kSEK**	**= 3 083 kSEK**
Total cash in project: (156+3 083)=3 239 kSEK, Total project volume: 7 707 kSEK			
* Corresponds to 2 021 kSEK at the time of writing this application			

2 Description of the plants

2.1 MEC MÅBJERGVÆRKET – SULFUR RECIRCULATION AND CORROSION MEMORY/ENVIRONMENT

The two municipalities Holstebro and Struer formed Vestkraft I/S, a federation of municipal and user-owned companies in West Jutland, Thy and Mors, started the construction work for Måbjergværket in April 1991, and in January 1993, the plant was put into operation. From the outset, the plant was far ahead of its time when it comes to climate issues, and today also contributes significantly to the fine climate accounts in the two municipalities. The planning and the plant have received both national and international awards for foresighted thinking.

In 1999 Vestkraft became a public limited company, and in the following year the company merged with other Jutland-Fyn power companies to Elsam A/S. At the big energy fusion in 2006, Måbjergværket was taken over by state-owned Ørsted. In the summer 2015, the CHP returned to local ownership. The plant is now owned by two utilities; respectively Vestforsyning - (owner share 5/7) and Struer Forsyning - (owner share 2/7).

Figure 3. Maabjergværket biomass and waste fired power plant

The plant consists of two waste fired boilers with a waste capacity of 2 * 11 metric tons/h and a Straw-/woodchips boiler firing 8/7 t/h. 180.000 t/year of household and industrial waste is treated in the waste lines together with 10.000 t/year of sludge. 26.000 t/year wood chips and 34.000 t/year of straw are fired in the third line.

The continuous electrical power output (net) is 28 MW and 84 MW of district heating power can be produced. 10 MW of the district heating is produced by flue gas condensation. 160.000 MWh/year of electricity is produced and 455.000 MWh/year of heat. The steam pressure is 64 bar and the steam turbine is designed for 520 °C, which is unusually high for a Waste-to-Energy plant. This high steam temperature is possible by an external gas fired superheater, which raises the steam from the

boiler superheaters from 412 to 520 °C. The two biogas fired superheaters consume 3,5 mio Nm^3/year.

The flue gas treatment of the waste fired boilers each consists of an ESP (Electrostatic Precipitator) and HCl scrubber supplied by ABB Fläkt. In 2004, both flue gas cleaning lines were retrofitted with an ADIOX/condensing/SO_2 scrubber supplied by Götaverken Miljö AB, now Babcock & Wilcox Vølund AB. The volumetric flow rate of the flue gas is 70,000 Nm^3/h (w.g.) (Figure 4).

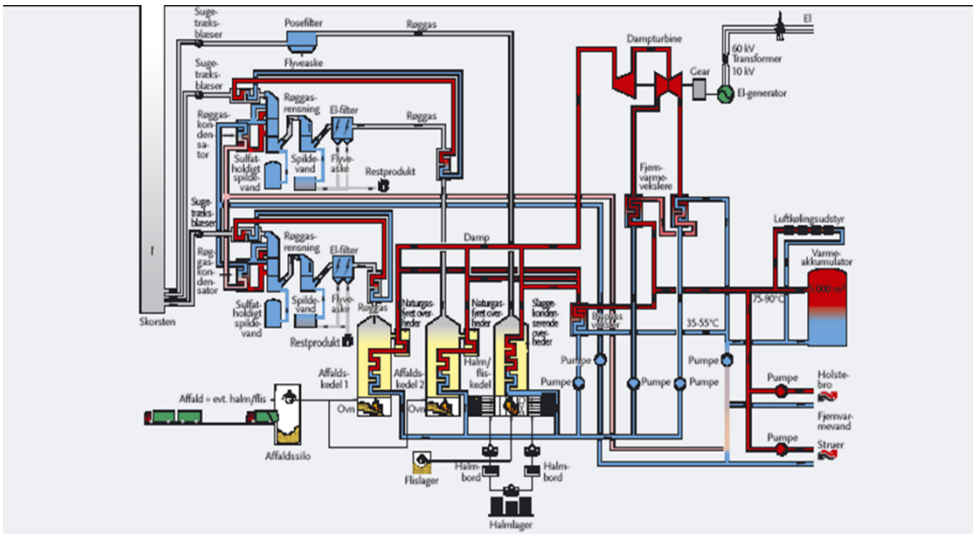

Figure 4. Simplified flow sheet of the MEC Maabjergværket biomass and waste fired power plant

2.2 AGED MATERIAL PROVIDED BY ØRSTED BIOENERGY & THERMAL POWER A/S - DTU COLLABORATION

Combustion of biomass in Danish decentralized CHP plants began in 1993, when the Danish government and utility operators made an agreement to use 1.4 mio. t. of biomass annually for power production in Denmark. This was mainly implemented in small decentralized grate fired CHP plants firing straw or wood chips. Currently, major efforts are made to implement large-scale use of biomass in central heat and power plants. This includes rebuilding of existing coal fired units or construction of new large flexible heat and power plants. Since the first use of biomass for heat and power production in 1993, a large number of in-situ tests of boiler materials have been carried out in Danish boilers in order to evaluate materials selection and corrosion rates as a function of steam temperature. The tests were carried out by utility companies in projects co-financed by Danish research programmes including both small grate fired boilers and co-firing of coal and biomass in large central power plants.

Systematic microstructure investigations of materials from in-plant tests were conducted from 1997 at the Technical University of Denmark (DTU) in close collaboration with the major Danish utility companies (ELSAM/ELKRAFT, ELSAM/Energi E2, Ørsted Bioenergy & Thermal Power A/S/Vattenfall). The aged material investigated comes from the collaboration between Ørsted and DTU and

other/previous DTU collaborations. Thus, a variety of field specimens from various boilers were available and from these, some were selected for investigation to give a deeper understanding of the evolution of microstructure from different fuels due to long term exposure.

Table 2: Summary of exposure parameters**Fel! Hittar inte referenskälla.** summarises the data on the exposed specimens investigated in this project. The steam temperatures cited are those available from the plant but the plant usually has varying temperatures around the reported steam temperature. The actual surface metal temperature is approximately 20ºC higher but depends on flue gas temperature, heat flux etc, and this data was not available. The different tubes are designated A (coal-firing), B and C (co-firing with biomass) and D, E and F (biomass firing).

Table 2: Summary of exposure parameters

	Fuel mix	Exposure time (hours)	Estimated steam Temperature (°C)	Pressure (bar)
A	Coal	27304	605ºC	210
B	Clean Wood pellets + oil	8397	568 ºC	150
C	Heavy oil + clean wood pellets + gas; coal fly ash additive + clean wood pellets;	54423 and 101100	Variable 520 -560	300
D	Wood chip firing	24500	495ºC	110
E	Wood and straw pellets	30535	Up to 540C	180
F	Straw	20401	555ºC	92

3 Experimental Conditions and material

3.1 MEC MÅBJERGVÆRKET – SULFUR RECIRCULATION AND CORROSION MEMORY/ENVIRONMENT

3.1.1 Sulfur Recirculation

Babcock & Wilcox Vølund AB in Sweden has installed their Sulfur Recirculation technology in one of the two Waste-to Energy lines at Maabjerg Energy Center (MEC) in Denmark in order to combat high temperature corrosion. This is the first commercial installation and it has been operating since mid-October 2016. Sulfur, separated in the wet flue gas treatment, is recirculated to and injected into the boiler, where it converts corrosive alkali chlorides to non-corrosive alkali sulfates as shown in Figure 5.

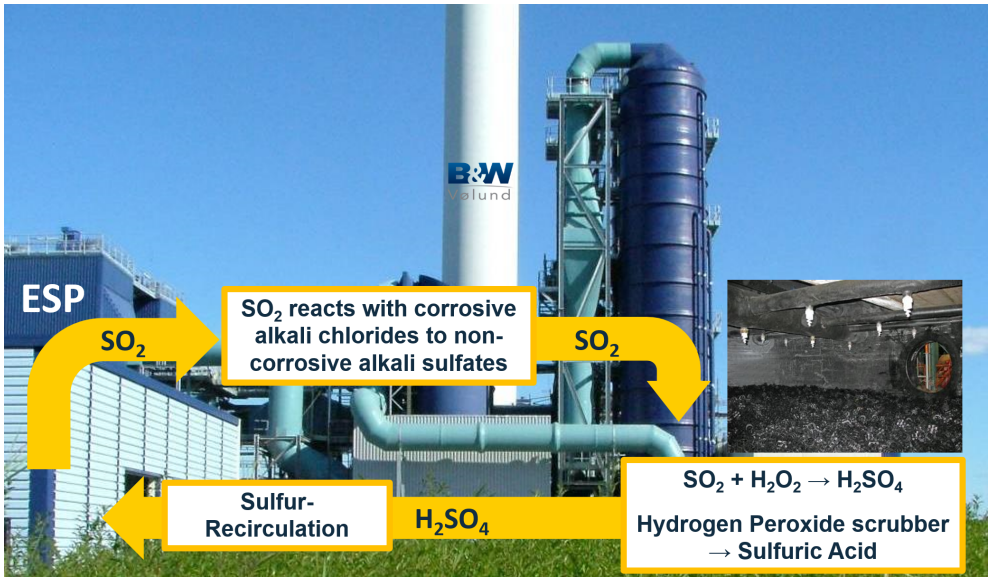

Figure 5: The flue gas treatment is seen together with the main chemical reactions. SO_2 is captured in the wet scrubber using H_2O_2 to produce H2SO4. The SO_2 concentration can now be maintained at a higher level, by dosing sulfuric acid into the furnace, which enables the alkali chloride to react to non-corrosive alkali sulfates.

The Sulfur Recirculation installation consists mainly of a storage vessel and dosage system for hydrogen peroxide (H_2O_2), a raw gas analyzer for SO_2, equipment for transport and dosage of sulfuric acid into the furnace. The sulfuric acid is sprayed through nozzles with atomization air, which produces a fine mist which evaporates rapidly. The dosage rate is controlled by a regulator, which maintains a fixed SO_2 setpoint. Previously, NaOH was used in both lines to produce a Na_2SO_4 solution which was transported away by road transport.

This is a unique opportunity to compare the corrosion rates in two parallel WtE combustion lines with the same fuel, but with and without Sulfur Recirculation respectively. The mean fuel composition was 29 wt% household waste, 63 wt% industrial waste 5 wt% sludge and 3 wt% wood waste, during the first year of operation (October 2016 – September 2017). The monthly mean waste composition

during the corrosion probe exposures (November 2016 – January 2017) ranged from 26-28 wt% household waste, 63-65 wt% industrial waste, 5-6 wt% sludge and 3 wt% wood waste, which is similar to the entire first year of operation.

3.1.2 Corrosion memory/environment - Probe exposures

The air-cooled corrosion study was performed during autumn 2016 and winter 2017 in the MEC boilers, see Figure 7. The exposures investigate the effect of the Sulfur Recirculation (SR) on the corrosiveness of the environment as well as the corrosion memory - environment effect. The memory effect is investigated by switching the probes between two different lines (boilers) where one has the Sulfur Recirculation installation and the other is a regular waste-fired line while one probe were exposed as reference in each line. The exposures were performed by air cooled probes consisting of two temperature zones (525 and 450 °C) and in total eight materials, see Figure 7. In order to reach the desired temperature, a cooling system is integrated in the probe and is based on air blowing the inside of the rings (blue arrow is the inlet for air and red arrow is the outlet).

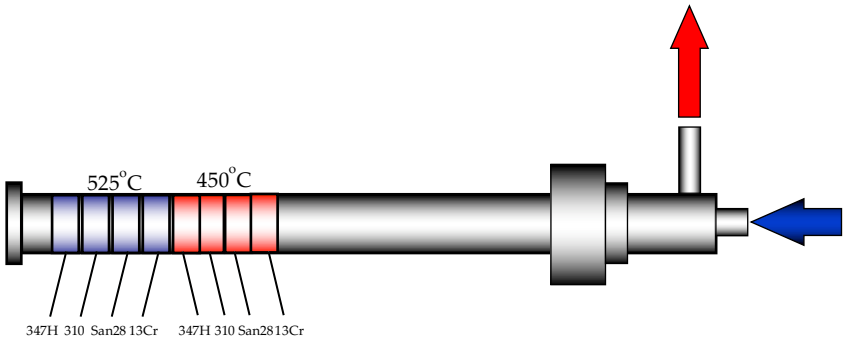

Figure 7. Schema of the probe used for the tests at Måbjergvaerket.

All exposures were performed with four different air-cooled probes:

- Two so called "reference probes" always stayed in their respective line during the whole duration of the exposure.
- Two so called "corrosion memory probes" were switched after half of the duration of the exposure.

A first set of experiments was performed in order to investigate the deposit formation during the first 48h. The corrosion memory probes were switched after 24h while the reference probes remained in their respective line during the whole 48h experiment, see exposure Table 3.

Table 3. Distribution of the probes in the different lines for the short term 48h exposure.

	Reference probe (Ref)	Reference sulfur (Rec)	Corrosion memory 1	Corrosion memory 2
Sulfur Recirculation Line (Rec)		48h	24h ↓	24h ↑
Reference Line (Ref)	48h		24h	24h

A second set of exposures were performed to study the long-time effect and consisted of a 2000h corrosion/deposit exposure using the same setup as described above, see Table 4.

Table 4. Distribution of the probes in the different lines for the long term 2000h exposure.

	Reference probe (Ref)	Reference sulfur (Rec)	Corrosion memory 1	Corrosion memory 2
Sulfur Recirculation Line (Rec)		2000h	1000h ↓	1000h ↑
Reference Line (Ref)	2000h		1000h	1000h

The materials used were: 13CrMo 4-5, 347, Sanicro 28 and 310 at both, 450 °C and 525 °C. Only the samples exposed at 525 °C are included in the report as the material loss measurements of the samples exposed at 450 °C showed very little material loss.

For practical reasons, below is the naming system of the samples:

Material – Line exposure 1, Line exposure 2

Material: Material investigated

Exposure line: Which line was used for the exposure. Rec being Line 1 with Sulfur Recirculation and Ref the reference Line 2 (without Sulfur Recirculation). For example: 347 Rec Rec means the sample of 347 exposed only in the line with Sulfur Recirculation. 347 Ref Rec means the sample of 347H exposed first in the line without sulfur (reference) and then, switched to the line with Sulfur Recirculation.

Table 5 shows the different SO_2 concentrations measured in both the Reference (Ref) and Sulfur Recirculation (Rec) lines during the corrosion probe exposures. There was a significantly higher SO_2 where there was Sulfur Recirculation.

Table 5: Summary of the corrosion probe exposure parameters (* SO_2 estimated from NaOH dosage).

		Exposure time (hours)	SO_2 dosage (mg/Nm^3, d.g.)	SO_2 concentration (mg/Nm^3, d.g.)
Ref	Reference	First 24 h	0	153*
Ref	Reference	Second 24 h	0	178*
Rec	Sulfur Recirc.	First 24 h	648	679
Rec	Sulfur Recirc.	Second 24 h	644	670
Ref	Reference	First 1000 h	0	265
Ref	Reference	Second 1000 h	0	190
Rec	Sulfur Recirc.	First 1000 h	511	601
Rec	Sulfur Recirc.	Second 1000 h	493	550

The materials investigated with the corrosion probe in MEC are presented in Table 6.

Table 6: Composition of the materials used in corrosions probes in wt.%.

	C	Cr	Ni	Si	Mn	Others
13CrMo4-5	0.08-0.18	0.7-1.15	-	<0.35	0.4-1	P<0.025 S<0.01 Mo 0.4-0.6
TP347H	<0.1	17.0-20.0	9.0-13.0	<0.75	<2.00	Nb 1.10
Sanicro 28	<0.020	27	31	<0.6	<2.0	P<0.025 Mo 3.5 Cu 1.0
310N	0.04-0.10	24.0-26.0	17.0-23.0	<0.75	2.0	Nb 0.2-0.6 Mo 1.10-1.50 N 0.15-0.35

3.1.3 Corrosion environment - Fixed installed superheaters

In order to perform long term exposures under realistic conditions, a number of different test materials were welded into the superheaters. In total, 8 test pieces, each with 6 different materials were welded into the two waste fired boilers. Two test pieces for each position times two superheater positions times two lines sums up to eight pieces. The two test tube positions of Line 1 with Sulfur Recirculation are marked with red ellipses. After half a year of operation, half of the samples were replaced with new 16Mo3 tubes and analyzed. After one year, the rest of the samples were analyzed. A photograph of the space between superheaters 2B and 1B2 (i.e. between the red ellipses in **Fel! Hittar inte referenskälla.**) is shown in Figure 9**Fel! Hittar inte referenskälla.**.

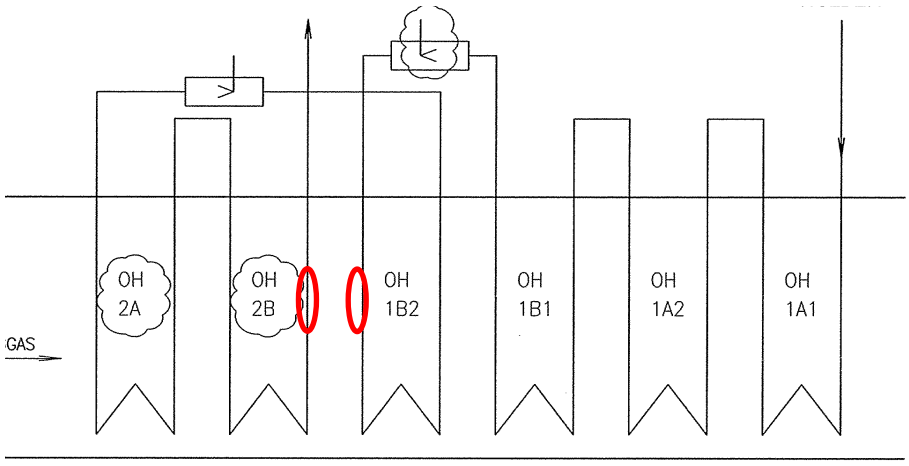

Figure 8. Test materials welded into the superheaters 2B and 1B2 of MEC Waste-to-Energy boiler K1 (Rec)

Figure 9. Test materials welded into the superheaters of MEC Waste-to-Energy boiler K1. Superheater 2B is to the right and superheater 1B2 is to the left. The gas flows from the right to the left.

The exposure times, steam production, flue gas temperatures and SO_2 concentration for each line and period are shown in Table 7 and Table 8. The material composition of the test materials is shown in Table 8 and Table 9.

Table 7. Summary of process conditions for the superheater material test with and without Sulfur Recirculation

		Exposure time (h)	Steam flow (t/h)	SO_2 dosage (mg/Nm^3, d.g.)	SO_2 conc. (mg/Nm^3, d.g.)
Ref	Reference first ½ yr	4053	40,7	0	225
Ref	Reference second ½ yr	3283	41,0	0	287
Rec	Recirc. first ½ yr	4008	40,7	477	530
Rec	Recirc. second ½ yr	4188	40,9	615	668

The steam flow was almost identical for the two lines in the respective period. The measured mean SO_2 concentration was 2.3 times higher with Sulfur Recirculation. The difference between the calculated SO_2 dosage into the boiler, and measured SO_2 concentration at the boiler outlet is quite small and is partly due to measurement inaccuracy and partly due to the fact that some of the sulfur ends up in the water treatment and is not recirculated back to the boiler.**Fel! Hittar inte referenskälla.**

Table 8. Summary of gas and steam temperatures in the superheater test positions.

	Line	Super heater	Gas temp (°C)	*Steam temp (°C)*
Ref	L2	2B	~550	Setpoint = 389
Ref	L2	3A	~530	Setpoint = 410
Rec	L1	2B	~530	Setpoint = 410
Rec	L1	1B2	~530	~330

For the position 2B, the gas temp and steam temperatures are within the same range

for both lines, but historically L1 has had higher corrosion rate which is likely due to the 20 °C higher steam temperature. 3A in L2 has similar conditions, while 1B2 in L1 has lower steam temperatures.

Table 9. Composition of the materials welded into the superheaters in wt.%

	C	Cr	Ni	Si	Mn	Others
16Mo3	0.16	0,16	0,15	0,28	0,70	P 0,01; S 0,002; Mo 0,31; Cu 0,27; V 0,003; Al 0,027
Sanicro 28 (Composite)	0.009	26.6	30.5	0.42	1.64	P 0.017; S 0.0008; Mo 3.32; Co 0.097; Cu 1.01; Al 0.03; N 0.051
W1.4841 (314)	0.06	24	20	1.9	1.7	P 0.02; S 0.0004
13CrMo4-5	0.13	0.9	0.03	0.26	0.53	P 0.006; S 0.004; Mo 0.48; Sn 0.002; Cu 0.04
3RE28 (Composite 310)	0,014	25.5	21.35	0.43	1.75	P 0.013; S <0.001; Mo 0.02; Ti 0.003; Cu 0.02; Al 0.034; Nb<0.01; N 0.097;
TP347H	0.07	17.4	10.2	0.27	1.09	P 0.033; S 0.007; Nb 0.85

3.2 CORROSION MEMORY/MICROSTRUCTURE - LABORATORY EXPOSURES

Two types of material were used to investigate the effect of ageing on high temperature corrosion mechanisms with KCl in the laboratory. The investigated material was a modified AISI 310 steel and a 347HFG steel with chemical composition as listed in Table 10.

Table 10. Composition of steels investigated wt.%.

	Cr	Ni	Cu	W	Mn	C	Si	Nb	V	Ti	N	Fe
Modified 310	23.8	22.0	2.77	2.46	0.84	0.088	0.023	0.36	0.36	0.27	0.03	Balance
Aged 347H *	19.7	12.5			1.5	n.m	0,7	0,5			n.m	Balance
As received TP347HFG*	19.8	10.7			1.6	n.m	0.52	0.65			n.m	Balance

*Measured with SEM-EDS

The modified 310 steel was specifically chosen for investigation because it develops widely different microstructures depending on heat treatment, i.e. containing a large fraction of σ-phase or almost no σ-phase.

The studies on 347HFG were conducted using samples prepared from aged or as received 347HFG steel tubes (Figure 10). The aged tube was a reheater tube from a coal firing power plant where the steam temperature was approximately 535 ˚C

exposed for 100,000 h [16]. The estimated surface metal temperatures were 585 ˚C on the flue gas side and 570 ˚C on the opposite side.

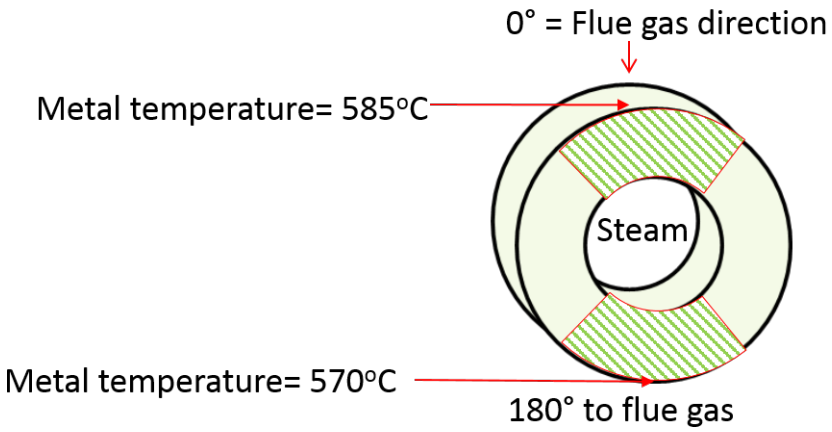

Figure 10: Locations of 0o and 180o aged samples, and sections used for corrosion testing.

Samples were exposed in a tube furnace equipped with a quartz tube to a 15 % (v/v) H_2O (g) + 5 %(v/v) O_2 (g) + N_2 (g) (balance) atmosphere at 600˚C for 168h. A schematic and full description of the experimental setup can be found in [17]. Exposures were done both with and without approximately 1 mm thick KCl deposit for both as received and heat-treated samples as described in

Table 11.

Table 11. Corrosion exposures undertaken under exposure environment

Material	Condition	Time and Temperature	Exposure environment
Modified 310	As-received	168 h, at 600ºC	5%O_2 + 15% H_2O + N_2
			5%O_2 + 15% H_2O + N_2 + KCl deposit
	Aged at 700ºC for 10,000 hours		5%O_2 + 15% H_2O + N_2
			5%O_2 + 15% H_2O + N_2 + KCl deposit
TP347H FG	As received		5%O_2 + 15% H_2O + N_2
			5%O_2 + 15% H_2O + N_2 + KCl deposit
	Exposed for 100000 hours in coal fired plant with steam temperature 535ºC		5%O_2 + 15% H_2O + N_2
			5%O_2 + 15% H_2O + N_2 + KCl deposit

3.3 CORROSION MEMORY/MICROSTRUCTURE - FIELD EXPOSURES

A variety of field specimens from various boilers were available from Ørsted/DTU. From these specimens some were selected for investigation to give a deeper understanding of the evolution of microstructure from different fuels due to long term exposure. Some of the samples were unique, already mounted and prepared water free and therefore could only be investigated with light optical and scanning electron microscopy. Other specimens could be investigated with etching techniques, and other techniques such as XRD and TEM. (Chemical etching is used

to reveal microstructure changes during the long ageing and corrosion process. However, etching removes water soluble corrosion products and the depth of corrosion attack, can appear greater after etching due to the preferential attack of grain boundaries. In addition, precipitates within the steel can be removed due to etching. Therefore, this process was not undertaken on unique specimens.) The specimens in all cases had been mounted in epoxy and polished to 1µm water free. If specimens were to be etched, water was used as a lubricant.

A tube from boiler F (see Table 2) was investigated where tubes had been removed consisting of both the exposed tubes from the boiler and a section from the penthouse (Figure 11). In this way, a comparison can be made from ageing and fireside corrosion. To be sure that the etchant was revealing an evolution in microstructure, two specimens were mounted together and etched together to make sure that the polishing and etching process was the same when comparing one specimen to another.

Figure 11: Tube examined for TP347H FG where section consists of both penthouse exposure and boiler exposure

The composition of steels investigated is given in Table 12.

Table 12: Composition of Materials investigated in wt.%

	C	Cr	Ni	Si	Mn	Others
Esshete 1250	0.06-0.15	14.0-16.0	9.0-11.0	0.20-1.0	5.5-7.0	Nb 0.75-1.25; V 0.15-0.40 Mo 0.8-1.2
TP347H	0.06-0.10	17.0-20.0	9.0-13.0	<0.75	<2.00	Nb 8xC <1.0
304HCu	0.07-0.13	17.0-19.0	7.5-10.5	<0.30	<1.0	Nb 0.3-0.6, Cu2,5-2,5 N 0.05-0.12, Al 0.003-0.030 B 0.001-0.010
310N	0.04-0.10	24.0-26.0	17.0-23.0	<0.75	2.0	Nb 0.2-0.6 Mo 1.10-1.50 N 0.15-0.35
Tempaloy AA1	0.07-0.14	17.5-19.5	9.0-12.0	<1.0	<2.0	2.0<(Ti+Nb/2)/C<4.0 B0.001-0.004 Cu2.5-3.5

The specimens were investigated with light optical and scanning electron microscopy. On one specimen, a FIB liftout and TEM analysis out was conducted at a region just below the corrosion front.

4 Analytical techniques

4.1 MEC MÅBJERGVÆRKET PROBES – SULFUR RECIRCULATION AND CORROSION MEMORY/ENVIRONMENT (HTC)

4.1.1 Qualitative analysis

All samples were investigated by visual inspection after exposure and documented by photographs. The colour, thickness and adherence of the deposit/corrosion product layer give rough information of the overall condition and performance of the exposed sample. All samples were stored in desiccators together with phosphorous pentoxide drying agent awaiting their analysis.

4.1.2 Scanning Electron Microscopy/Energy Dispersive X-Rays (SEM/EDX)

After the boiler exposure, the samples were casted in epoxy, cut and polished prior to the SEM/EDX investigation. The rings were casted by first descending them in epoxy resin. Both sample and mould were then subjected to a 10-bar pressure to avoid the formation of bubbles during the hardening of the resin. The hardening time was fixed in 24 hours. After the hardening of the epoxy resin was complete, the samples were cut using a silicon carbide disc and a lubricant without any water due to the delicate corrosion products. The samples were then polished dry with Silicon Carbide P4000. The cross-section was coated with gold to avoid charging in the SEM. The polished cross-sections of the samples were investigated by scanning electron microscopy, SEM. The SEM is equipped with an Energy Dispersive X-ray system enabling analysis of the elemental composition in small areas of the sample. In this study, a FEI 200 Quanta FEG ESEM was used. It is equipped with a field emission electron gun (FEG) and an Oxford Inca energy dispersive X-ray (EDX) system. SEM/EDX was used for imaging, elemental mapping and quantification. An accelerating voltage of 20kV was used for all analysis.

4.1.3 Material loss measurements

The samples were evaluated by means of metal loss determination. The material loss of the Superheater samples was performed with an Olympus 38DL Plus ultrasonic thickness gauge with a 0.01mm resolution was used for the measurements. The material loss measurements of the ring samples were performed with SEM.

4.1.4 Ion Chromatography (IC)

To determine the amount of water-soluble anions (Cl^-, SO_4^{2-}) on the deposit of the exposed samples, a Dionex ICS-90 system was used. The anions were analysed with an IonPac AS4A-SC analytic column and 1.8mM NaHCO3/1.7mMNaHCO3 was used as eluent. The flow rate was 2ml/min. A representative and known amount of deposit was removed from the samples and dissolved in 100 mL distilled water. A 5 mL sample of this prepared solution was inserted into the IC column in order to know the amount of chlorine and sulfate ions (ppm). The results are presented as mass percentage (amount of ions/100 g deposit).

4.1.5 ICP-MS

The ICP-MS analyses of the deposits were performed by Eurofins Environment Testing Sweden AB, which are accredited by Swedac SS-EN ISO/IEC 17025. The sample preparation was made according to EN 14780-11/EN 15443-11/SS 187114-92/SS 187117-97. The chloride concentration was analysed according to SS 187185 and the other elements were analysed according to EN13656 and EN14385.

4.2 CORROSION MEMORY/MICROSTRUCTURE PROBES – LABORATORY AND FIELD EXPOSURES (DTU/ØRSTED)

Cross-sections of corrosion tested samples were cold mounted in epoxy to ensure a tight embedding and to preserve the corrosion products. The sintered salt was removed before embedding to reduce the risk of smearing during grinding and polishing. The mounted samples were ground up to 4000-grit SiC paper followed by polishing using 3μm and 1μm diamond paste and absolute ethanol (water free, 99.99%) as lubricant to reduce dissolution of the chlorine containing corrosion products.

Characterization was conducted with reflected light optical microscopy (RLM), scanning electron microscopy (SEM/EDX), X-ray diffraction (XRD) and transmission electron microscopy (TEM/EDX). FIB-milling using a FEI Helios Nanolab was used to lift out a TEM sample from the internal corrosion front from the corrosion exposed heat-treated sample. As a complement to TEM-EDX quantitative analysis, a qualitative Cr content analysis using electron energy loss spectroscopy (EELS) was performed at the corrosion front. The EDX measurements for oxygen have a lower accuracy, and therefore the values should be assessed with caution.

Thermodynamic calculations were performed using Thermo-Calc software version 2016b [20] using the Thermo-Calc Software TCFE6 Steels/Fe-alloys database version 6.1 to predict phase amounts and compositions of thermodynamically stable phases as a function of temperature.

5 Results

5.1 MEC MÅBJERGVÆRKET – SULFUR RECIRCULATION AND CORROSION MEMORY/ENVIRONMENT

5.1.1 Sulfur Recirculation – general observations

After the initial project delay, which was due to MEC changing owners, the installation project went according to plan. The change of desulfurisation agent from NaOH to H_2O_2 was tested just before the planned maintenance stop in the autumn of 2016 in order to produce some sulfuric acid for the startup of Sulfur Recirculation. After the maintenance stop, when the super heater test materials were welded into the full-scale superheater, the Sulfur Recirculation system was put into operation and has been operating since then, only with minor interruptions.

After a year of operation, Sulfur Recirculation had almost completely eliminated the need for costly transport and disposal of residual sulfate water, since the excess sulfur now ends up in the fly ash. Simultaneously, the emissions of dioxins and CO in the flue gas were reduced.

5.1.2 Deposit formation in the superheater region – air cooled probes

General observations

The deposits observed on the different air-cooled probes is shown in Figure 12. The deposits acquired on the recirculation line exhibited a slightly higher hardness than the reference line. This could be seen by the resistance of the deposits when the probes were removed/samples removed.

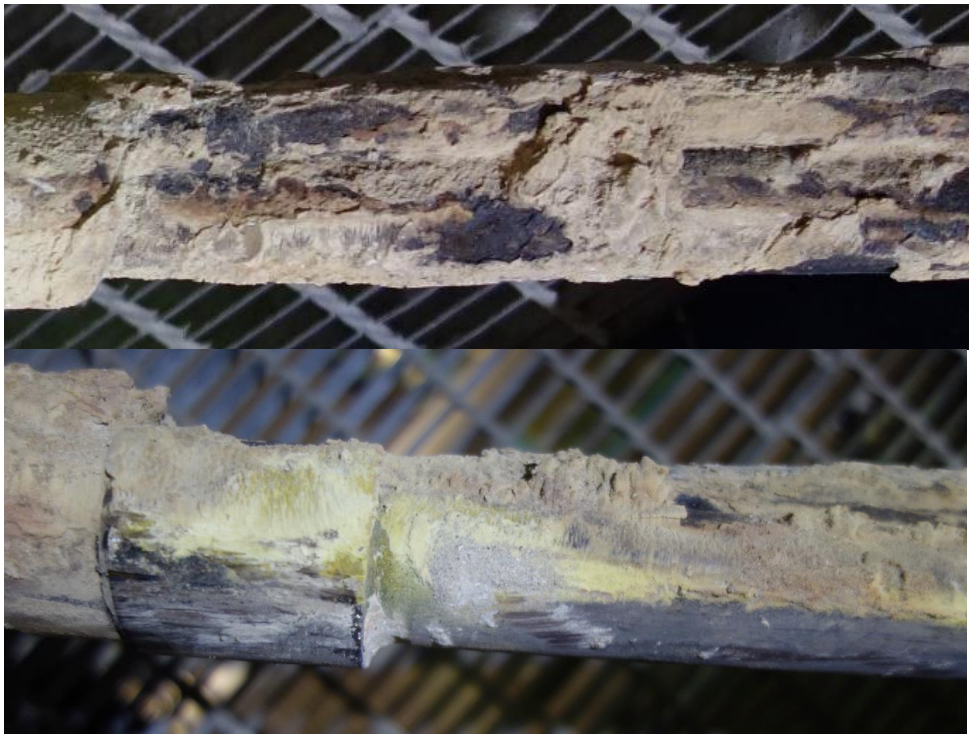

Figure 12. Photographs of the corrosion probes after 1000 + 1000 h Ref (top) and 1000 + 1000 h Rec (lower).

Deposit composition - IC

In order to analyse the deposit composition in the superheater region, some deposit was removed from the air-cooled probes before the removal of the samples. All the deposits were hard and difficult to remove from the probes, see example in **Figure 13**.

Figure 13. Probe exposed 1000h in the Sulfur Recirculation line (first) and 1000h in the reference line (after)

The amount of chlorine and sulphate was determined by means of ion chromatography as it was described in section 4.1.4. Figure 14 shows the percentage of chlorine in the deposit for the different exposures. After 48h the amount of chlorine in the deposit is 31% lower in the Sulfur Recirculation line and after 2000h the reduction of the chlorine is drastic between the Sulfur Recirculation line and the reference line (waste) with a 97% reduction of chlorine in the Sulfur Recirculation line. The amount of chlorine in the reference line was about 2,65% and 0,1% in the Sulfur Recirculation deposit. Regarding the corrosion memory probes which were

exposed 1000h in each line/environment, there were a large spread in the results. The dense hard deposits made it very difficult to remove a representative part of the deposit. As a result of this analysis, those samples may only reflect the composition of the most external deposit, i.e. only for the last 1000h.

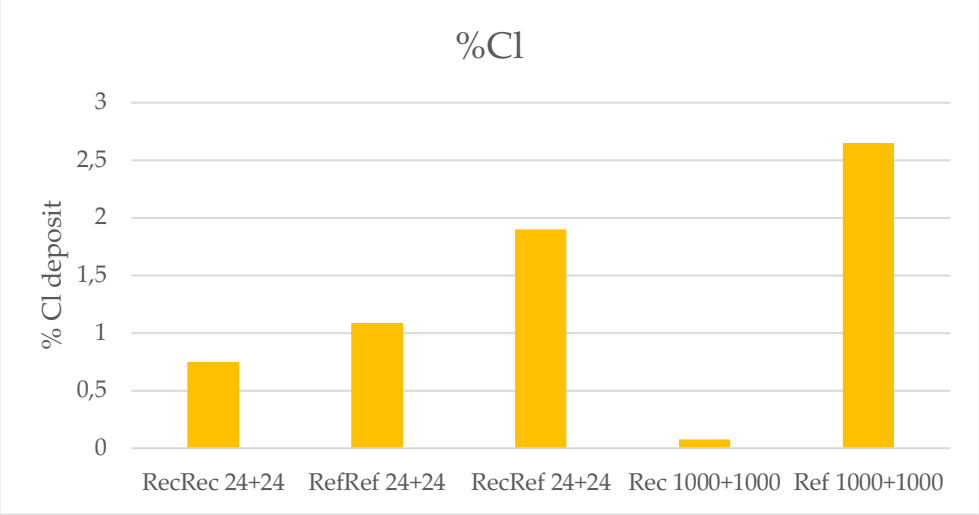

Figure 14. Percentage of chlorine in the different deposits. Line 1 = Rec, Line 2 = Ref.

The Figure 15 shows the percentage of sulfate in the deposit for the different test conditions. After 48h no clear difference can be seen between the different lines. After 2000h exposure the amount of sulfur in the Sulfur Recirculation line is 25,5% while in the reference line is only 9%. As with the chlorine measurements of the deposits, the hard deposits made it very difficult to take a homogeneous deposit sample of the corrosion memory probes. Therefore, only the results for the separate lines are presented.

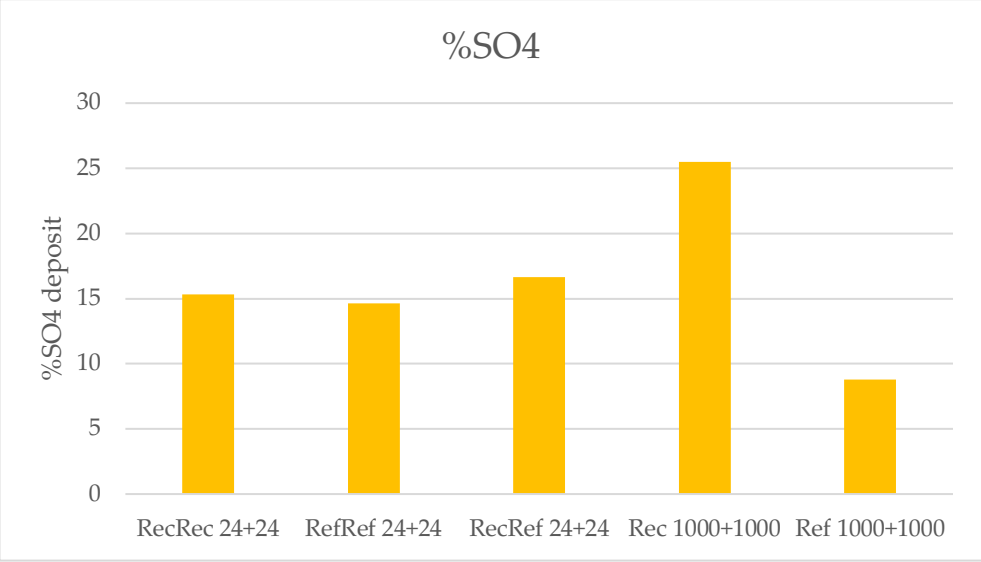

Figure 15. Percentage of sulphate in the different deposits Line 1 = Rec, Line 2 = Ref.

5.1.3 Deposit formation in the superheater region - fixed installed superheaters

General observations

It has been reported elsewhere that deposit rate decreases with higher sulfur concentration [1]. Until now, two planned maintenance stops have been made after Sulfur Recirculation was taken into operation. At both these locations the deposits formed in the superheater were slightly harder and more difficult to remove in the Sulfur Recirculation line than the reference line. However, the deposit formation did not cause any shortening of the operating periods between the planned stops. The cause is currently being investigated. One explanation could be that the gas temperature was higher than usual in the superheaters of the Sulfur Recirculation line.

The deposits formed on the corrosion probes during both the reference and Sulfur Recirculation exposures were all extremely hard and difficult to remove for analysis after: see example in **Figure 16**. An angle grinder was used in order to remove the deposit locally and measure the material loss by using ultrasound.

Figure 16. Superheater after 6 months in Sulfur Recirculation line

Deposit composition

The composition of the corrosion probe deposits analysed with IC is compared to the fixed super heater 2B deposits, analysed with ICP-MS. The Superheater 2B position is exposed to the same gas as the corrosion probes.

Table 13. Percentage (wt%) of chlorine in the corrosion probe (IC) vs. fixed superheater (ICP-MS).

	Deposits on corrosion probe after 2 x 1000 h	Superheater 2B deposits after ½ year of operation
Ref	2,65	1,84
Rec	0,08	0,27

An example of the removed deposit is shown in **Figure 17**.

Figure 17. Piece of deposit extracted from the Sulfur Recirculation line after 2000h exposure

Table 14: ICP-MS analysis of the superheater deposits in position 2B of Ref (L2) and Rec (L1) after the first ½ year of operation.

Exposure time (hours)	Ref (L2) wt% DS	Rec (L1) wt% DS
Cl	1,84	0,27
S	20	19
Ca	11	10
Na	8,8	7,9
K	5	2,1
Si	1,9	1,3
Al	1,2	1,2
Fe	1,1	1,8
Other	3,0	2,8

As already shown in Table 13, the most dramatic difference between the composition of the superheater deposits is the chlorine concentration, which was 6.8 times lower with Sulfur Recirculation, but also the alkali concentration was lower. This could possibly be attributed to less condensation of gaseous alkali chlorides onto the superheaters or less sticky particles due to lower alkali chloride content.

5.1.4 Corrosion in the superheater region – air cooled probes

The corrosion rates were investigated by air cooled probes during the initial and medium long exposure times (1000 + 1000h) in the superheater region. The exposure scheme described was described in section 3.1.3 generated in total 64 samples. All samples were documented regarding deposit formation, optically investigated (IC and photos as described above) and material loss measured. Based on the initial investigation the most interesting samples were in addition investigated in detail by SEM/EDX.

Material loss

The samples exposed the longest time (1000h + 1000h) at the higher temperature (525 °C) were measured in terms of material loss. Figure 18 shows the average material

loss calculated for the total 2000h exposure. Both Sanicro 28 and 310 samples show very little or no measurable material loss in all the different conditions.

The 347H samples show some material loss and a difference between the reference line and the Sulfur Recirculation line could be observed, see Figure 18. The sample exposed in the reference line (waste) during 2000h presents a 0,05-mm material loss compared with the negligible material loss of the sample exposed 2000h in the Sulfur Recirculation line. The sample exposed 1000h in the Sulfur Recirculation line (first) and 1000h in the reference line (after), presents a considerable less material loss (0,03 mm) than the one exposed only in the reference line, but more than the one exposed in the Sulfur Recirculation line. This indicates a positive corrosion memory effect of the sulfur rich environment/deposit for the 347H material. In line with these results the sample exposed first 1000h in the reference line and 1000h in the Sulfur Recirculation line showed a higher material loss than the reference sample indicating a corrosion memory effect also in this case.

In the case of the 13CrMo4-5 samples is it possible to observe similar a memory effects. The reference sample (2000h in the waste line) presents the biggest material loss of all of them while the Sulfur Recirculation sample (2000h in the Sulfur Recirculation line) shows the lowest value. The combined samples (1000h in each line) present intermediate values in both cases, indicating a positive memory effect.

The 347H and 13CrMo4-5 were selected for a further material loss and SEM/EDX analysis as they are the most promising samples in order to analyze the difference between the different exposure conditions as well as the memory effect.

Both Sanicro 28 and 310 showed very little corrosion even in the most corrosive environment and no further analysis were performed on these alloys as no difference can be measured between the different environments.

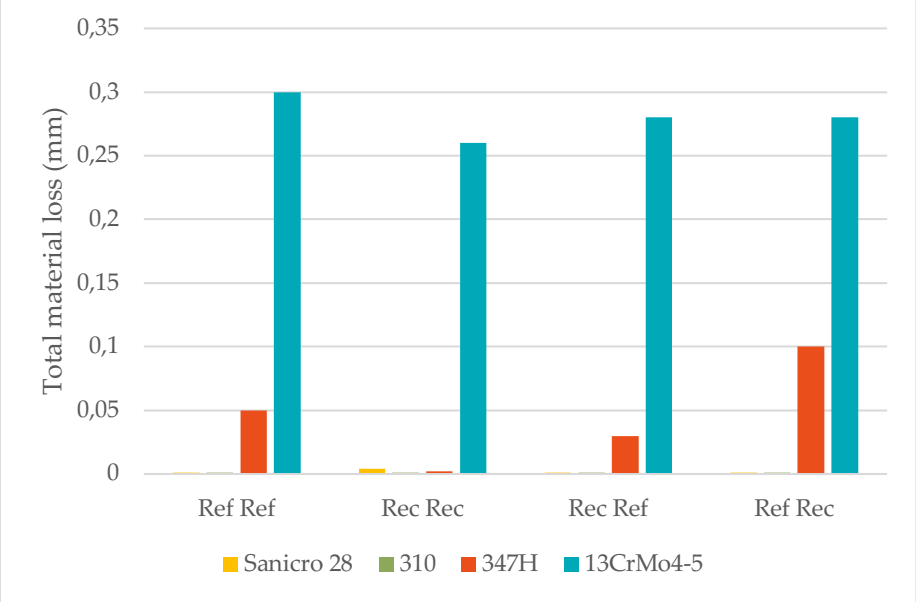

Figure 18. Material loss of the samples exposed 2000h at 525°C

The material loss was in addition measured in profile around the sample ring for the 347 and 13CrMo4-5 samples exposed at 525 °C for 2000h, i.e. the samples that showed the highest material loss, see Figure 19.

At 525 °C after 2000h exposure the Sulfur Recirculation shows a positive effect on the 347H materials corrosion rate. The samples 347 Rec Rec and 347 Rec Ref have a lower material loss than the sample 347 Ref Ref. The diagrams in addition show that the material loss of 347 and 13CrMo4-5 is non-uniform and higher on the flue gas side.

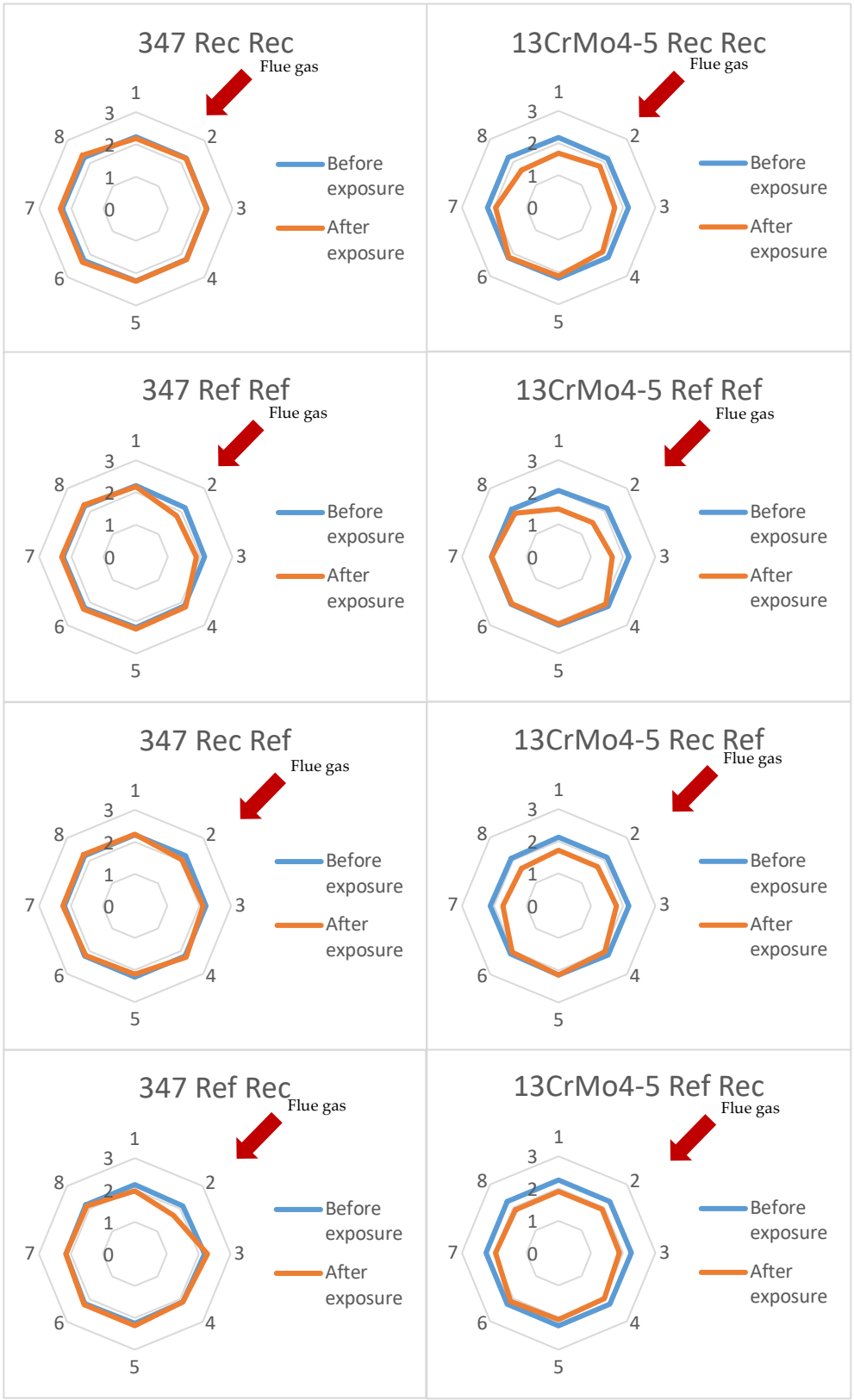

Figure 19: Material loss after corrosion tests of 347 and 13CrMo4-5 at 525°C and 2000h. The red arrow marks the flue gas direction relative the ring.

Figure 20 shows in detail the effect of the Sulfur Recirculation in the 347H material at 525°C by presenting the maximum material loss (mm/year) of the samples after being exposed in the different lines. The left part of the graphic shows the reduction in material loss of the 347H material being exposed only in the waste line (reference) compared with the material only exposed in the Sulfur Recirculation line. The decrease in material loss is 89% showing a clear positive effect of the Sulfur Recirculation.

The right part of the graphic presents the reduction in material loss of the samples exposed only in the waste line compared with the samples exposed first in the Sulfur Recirculation line during 1000h and then in the reference line during 1000h. The reduction of material loss is 60% showing a positive corrosion memory effect when exposing the samples first in the Sulfur Recirculation line.

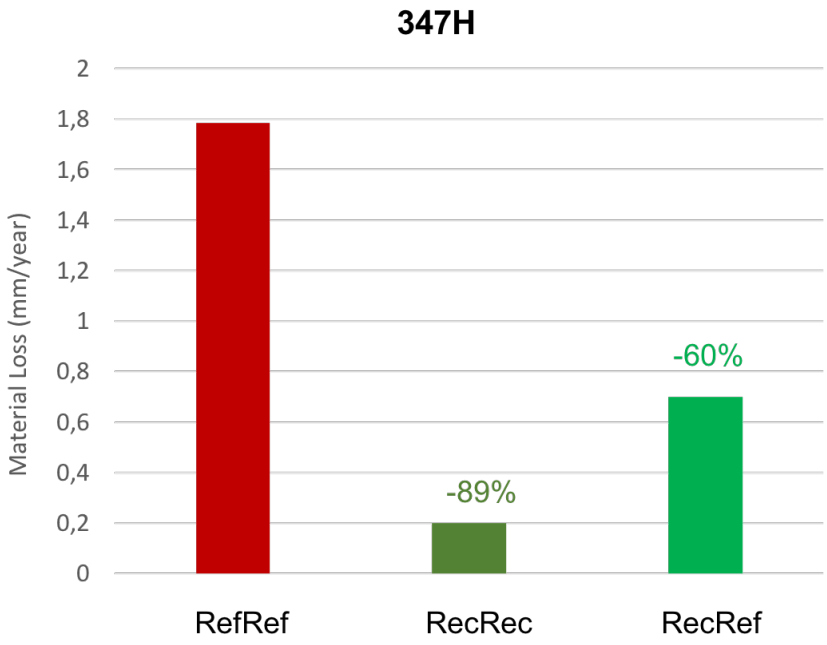

Figure 20. Effect of the max material loss in mm/year on Sulfur Recirculation for the 347H material

Deposit/oxide microstructure – SEM/EDX

The 347 and 13CrMo4-5 samples exposed at 525 °C for 2000h were selected for a more detailed investigation. The samples were casted in epoxy, cut, polished and investigated via SEM.

- 347H exposed to waste at 525 °C for 1000h + 1000h (Ref Ref)

The samples exposed in the waste line represents the environment without the installed Sulfur Recirculation. **Figure 21** shows low magnification SEM/BSE images of the cross-section. Most of the deposited/corrosion products spalled of during sample handling. The images illustrate the difference in corrosion attack on the different sides of the ring indicated in material loss measurements, see Figure 19.

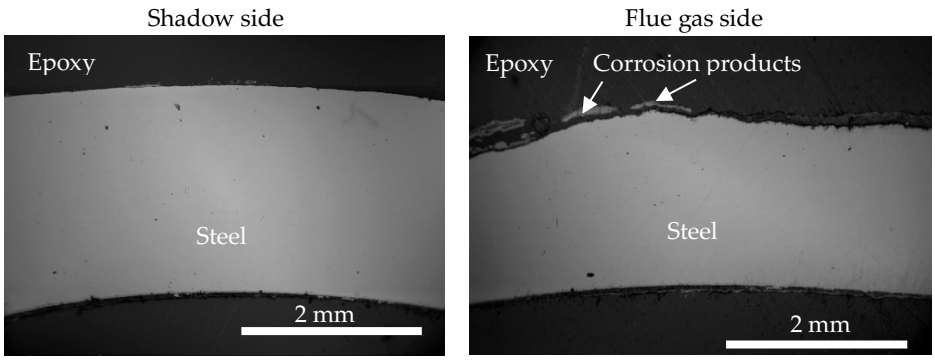

Figure 21:BSE image showing a low mag cross section of 347 Ref Ref at 525 °C for 2000h.

Corrosion products can be observed on both side of the sample, shadow and flue gas side. However, the flue gas side exhibits signs of steel grain boundaries attack (**Figure 22**).

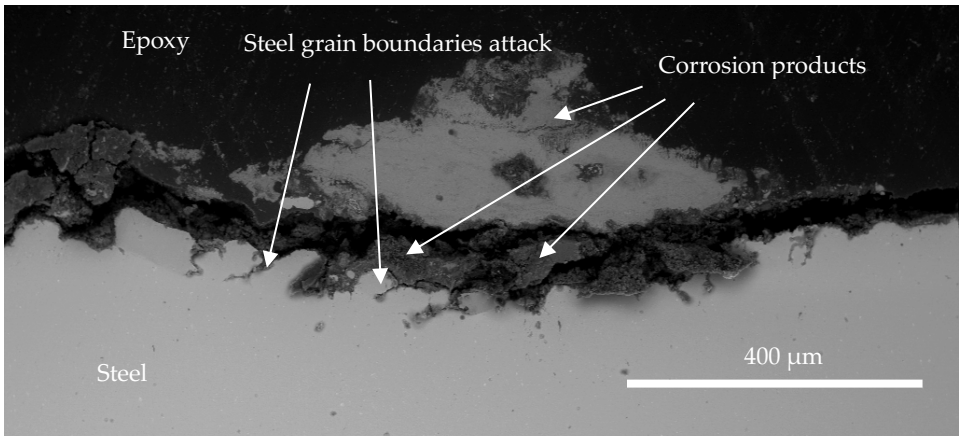

Figure 22: BSE image showing a high mag cross section of the flue gas side of 347 Ref Ref at 525 °C for 2000h.

The EDX analysis from the most corroded side in **Figure 23** shows that the corrosion products are mostly made of chromium and iron rich oxide. The nickel tends to stay at the interface metal/oxide or the corrosion front where the steel grain boundaries attacks are located. No traces of potassium nor sulfur were detected in good agreement with the IC results in Figure 15 as the line 2 shows the least amount of sulfur. Large amount of chlorine/metal chlorides was observed at the interface metal/oxide which also correlates well with the IC results in Figure 14 from line 2 (ref).

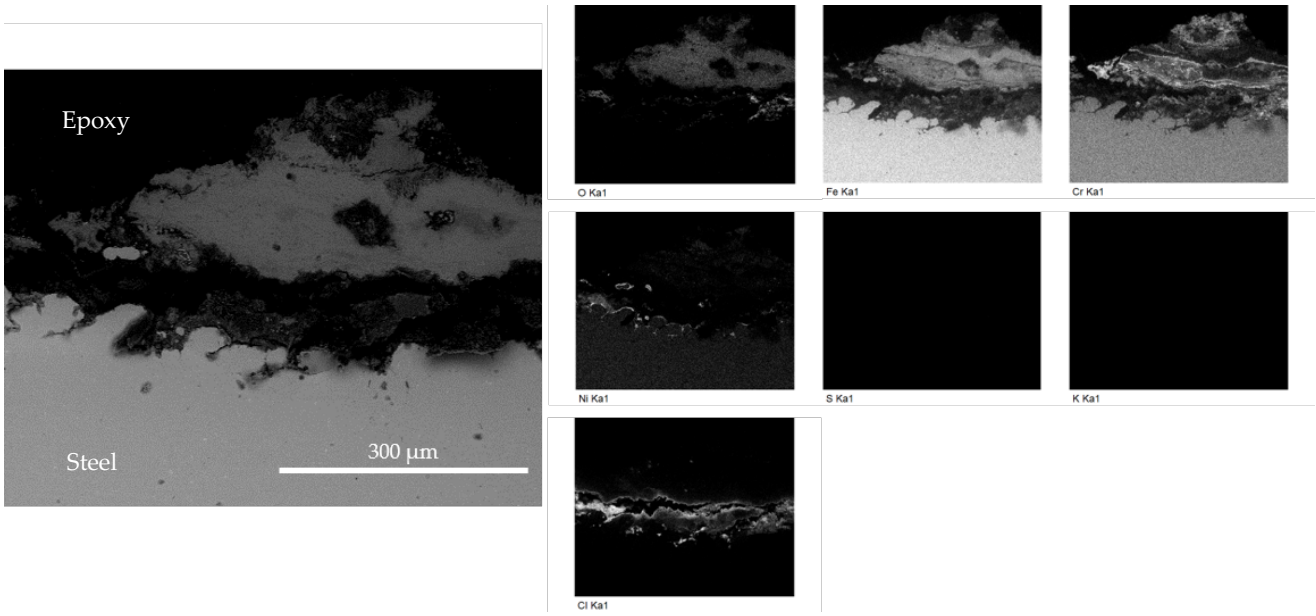

Figure 23: EDX analysis of the flue gas side of 347 Ref Ref at 525 °C for 2000h.

- 347H exposed to waste + SR at 525 °C for 1000h + 1000h (Rec Rec)

In the case of 347 Rec Rec (2000h in Sulfur Recirculation line reference), almost no material loss could be observed. The SEM images is in good agreement and the overall thickness of the reference sample 347 Rec Rec, seems homogeneous and not heavily corroded (Figure 24: BSE image showing a low mag cross section side of 347 Rec Rec at 525 °C for 2000h.). Small amounts of deposits remain on top of the shadow side could be observed while in the flue gas side case, it spalled off due to sample handling. The surface of the bulk material is smoother on the shadow side. The material loss on the flue gas side for 347 Rec Rec is lower than for 347 Ref Ref, No steel grain boundaries attacks are observable for 347 Rec Rec as in the case for 347 Ref Ref.

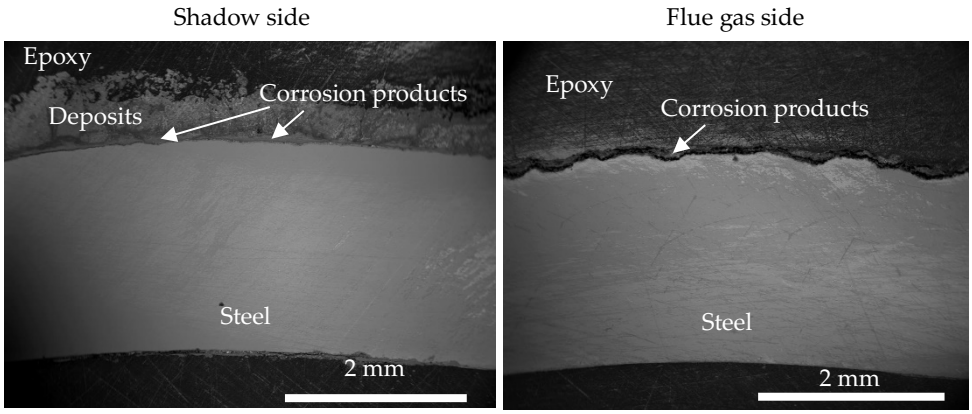

Figure 24: BSE image showing a low mag cross section side of 347 Rec Rec at 525 °C for 2000h.

The EDX analysis presented in **Figure 25: EDX analysis of the flue gas side of 347 Rec Rec at 525 °C for 2000h.** shows that the oxide is mainly constituted of a chromium, nickel and iron spinel oxide. No traces of potassium can be seen, while the presence of sulfur is observable. This is expected based on the Figure 15 as the line has the Sulfur Recirculation installation. Chlorine was detected along the interface metal/oxide as well as nickel.

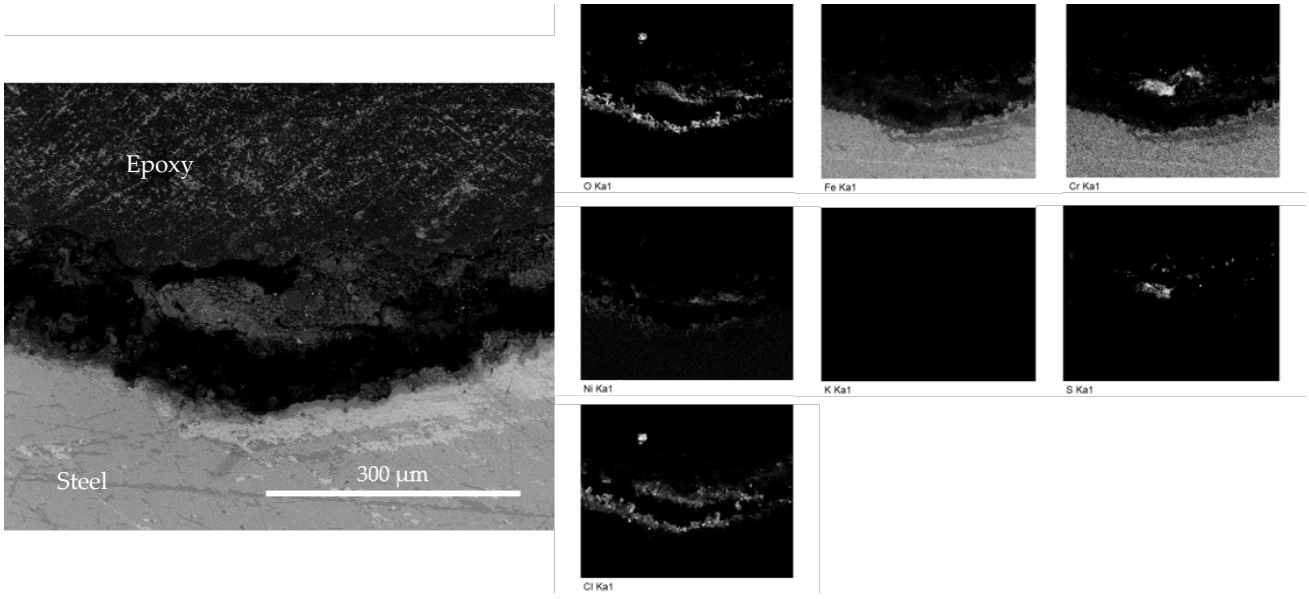

Figure 25: EDX analysis of the flue gas side of 347 Rec Rec at 525 °C for 2000h.

- Corrosion memory 347: waste + SR 1000h - waste 1000h at 525 °C (Rec Ref)

In the case of the corrosion memory sample 347 Rec Ref (1000h in Sulfur Recirculation line first + 1000h in reference line), some material loss could be observed on the flue gas side of the sample, but less than the sample exposed only

in the reference line (347 Ref Ref) which has a material loss of 170 μm on the flue gas side.

The **Figure 26: BSE image showing a low mag cross section of 347 Rec Ref at 525 °C for 2000h.** shows that most of the deposits spalled off due to sample handling, as it can be seen on those two pictures. The shadow side seems to have a smoother surface than the flue gas side, and a lower material loss. This is in agreement with the Figure 19 showing the material loss.

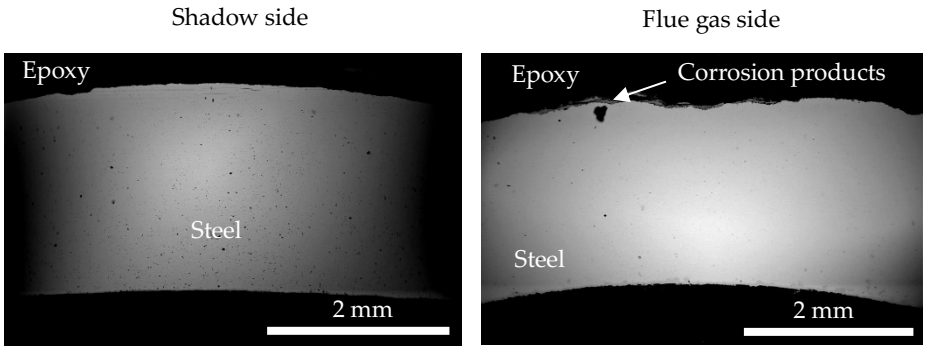

Figure 26: BSE image showing a low mag cross section of 347 Rec Ref at 525 °C for 2000h.

No deposited can be observed due to spallation while some parts of oxide remain on top of the material with an average thickness of ~ 50 μm.

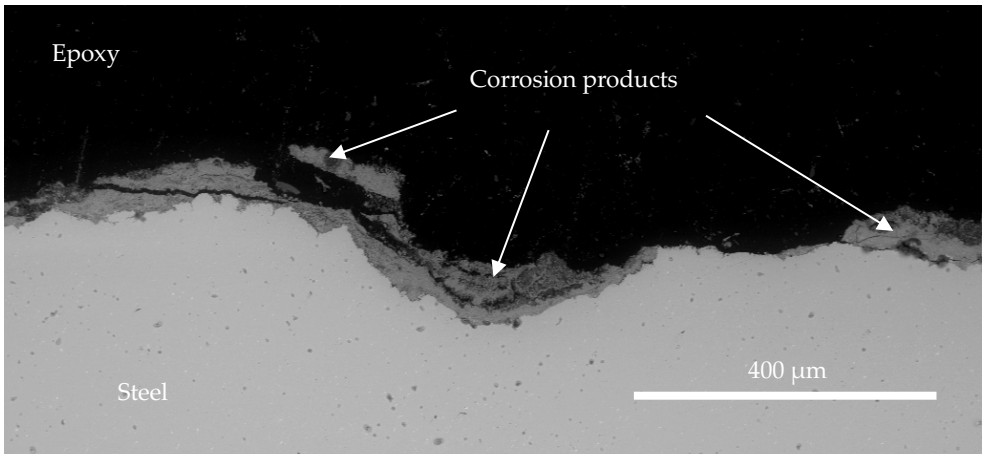

Figure 27: BSE image showing a high mag cross section of the flue gas side of 347 Rec Ref at 525 °C for 2000h.

The EDX analysis presented in **Figure 28: EDX analysis of the flue gas side of 347 Rec Ref at 525 °C for 2000h.** shows a layer of $(Fe,Cr,Ni)_3O_4$ oxide. No potassium detected, but some traces of sulfur and chlorine can be observed at the interface metal/oxide

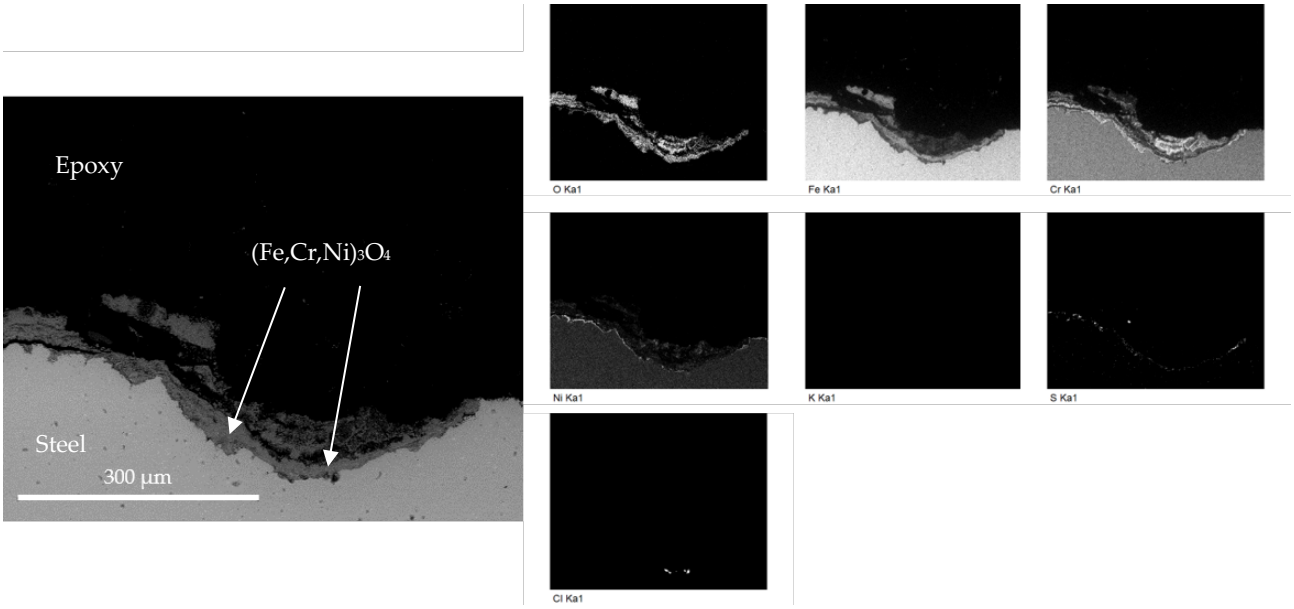

Figure 28: EDX analysis of the flue gas side of 347 Rec Ref at 525 °C for 2000h.

- Corrosion memory 347: waste 1000h - waste + SR 1000h at 525 °C (Ref Rec)

The corrosion memory sample 347 Ref Rec (1000h in reference line first + 1000h in Sulfur Recirculation line is presented in **Figure 29**. It shows that the shadow side have remaining deposits on top of the oxide while on the flue gas side it has spalled off. The surface of the shadow side looks also smoother than the flue gas side and with less material loss, which agrees with the Figure 19.

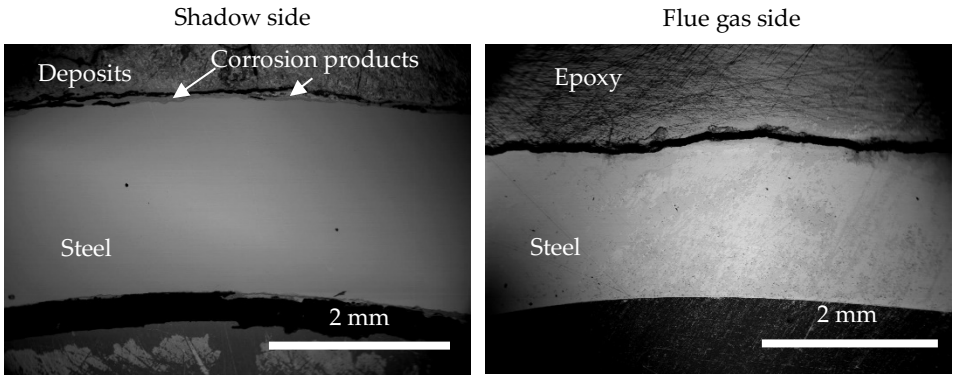

Figure 29: BSE image showing a low mag cross section of 347 Ref Rec at 525 °C for 2000h.

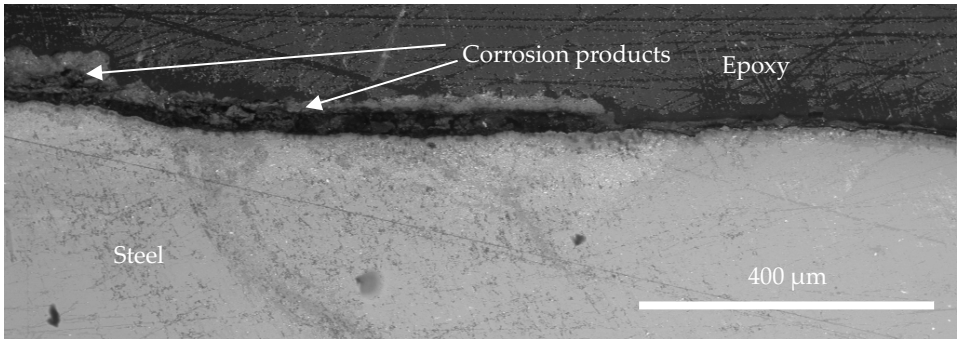

Figure 30: BSE image showing a high mag cross section of the flue gas side of 347 Ref Rec at 525 °C for 2000h.

The EDX analysis presented in **Figure 31** shows a thin layer of iron oxide laying on top of the material. A great amount of chlorine is also observed on top of the material, while no potassium nor sulfur were observed.

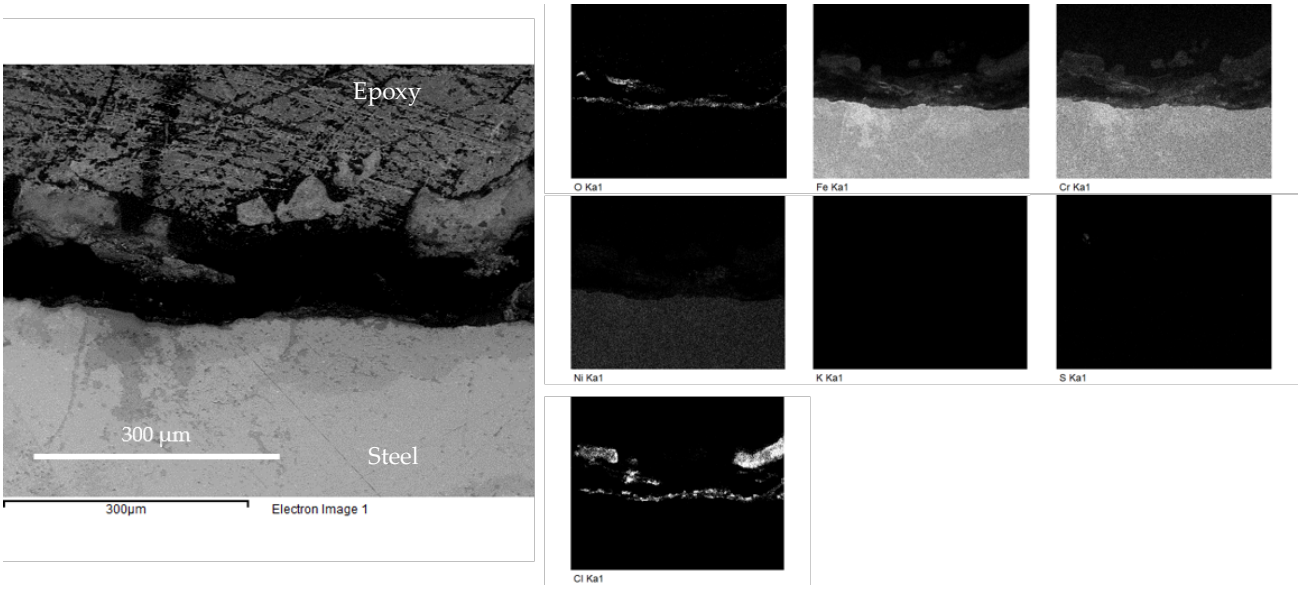

Figure 31: EDX analysis of the flue gas side of 347 Ref Rec at 525 °C for 2000h.

Deposit/oxide microstructure of the low alloyed steel 13CrMo4-5 – SEM/EDX

In the case of 13CrMo4-5 Rec Rec (2000h in Sulfur Recirculation line) and 13CrMo4-5 Ref Ref (2000h in reference line reference), the line with sulfur shows an average material loss of 390 µm while the line without sulfur has an average of 573 µm.

- 13CrMo4-5 exposed to waste + SR at 525°C for 1000h + 1000h (Rec Rec)

The **Figure 32** show BSE images of the reference sample 13CrMo4-5 Rec Rec. The shadow side shows no severe corrosion attack and its deposits fell off during the handling of the sample. The flue gas side show oxides of ~ 120-340 µm on top of the material that were broken during sample preparation. The shadow side exhibits a lower material loss than the flue gas side as expected in Figure 19.

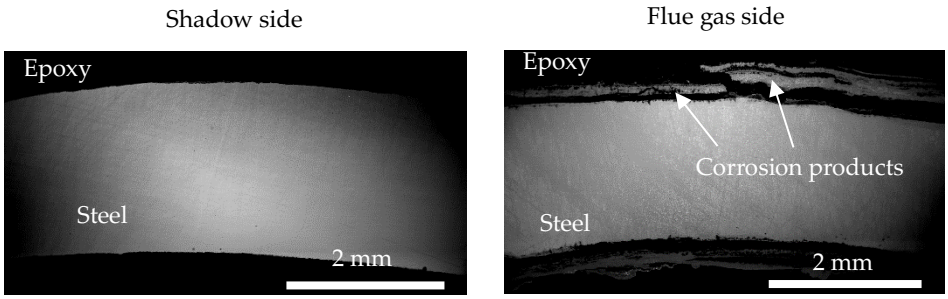

Figure 32: BSE image showing a low mag cross section of 13CrMo4-5 Rec Rec at 525 °C for 2000h.

The EDX analysis presented in **Figure 33** exhibits black dots on the steel part due to the use of oil during the sample preparation. A broken layer of ~ 120-210 µm of iron oxide is observed, while of chlorine is detected on top of the material and between the different broken oxide layers. Sulfur is detected within the iron oxide layers.

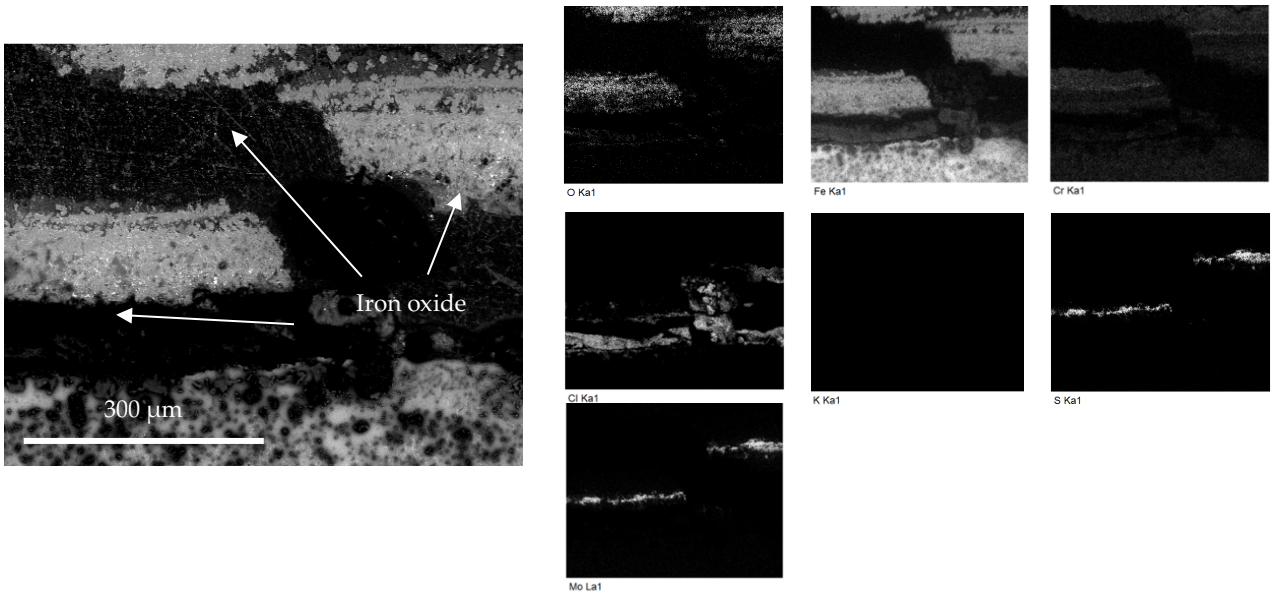

Figure 33: EDX analysis of the flue gas side of 13CrMo4-5 Rec Rec at 525 °C for 2000h.

- 13CrMo4-5 exposed to waste at 525 °C for 1000h + 1000h (Ref Ref)

The **Figure 34** from sample 13Cr Ref Ref shows the same feature as sample 13Cr Rec Rec. No severe corrosion on the shadow side and oxides of ~ 410 µm on top of the sample coupled with a lower material loss on shadow side, which agrees with Figure 19. The black spots are oil spots.

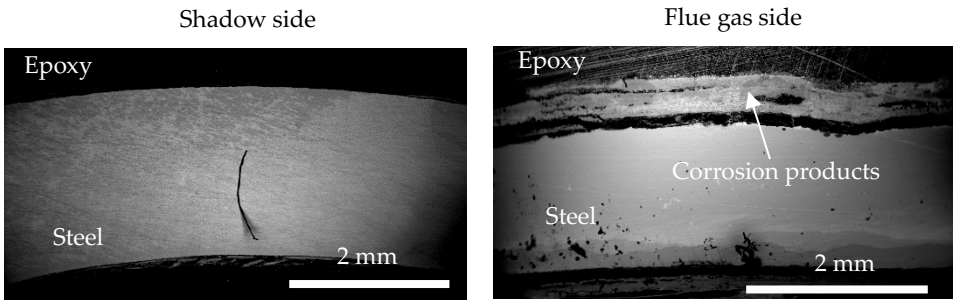

Figure 34: BSE image showing a low mag cross section of 13CrMo4-5 Ref Ref at 525 °C for 2000h.

The EDX analysis represented in **Figure 35** shows that mainly iron oxide is present. Chlorine was detected at the interface metal/oxide. Traces of sulfur and potassium can also be seen within the oxide.

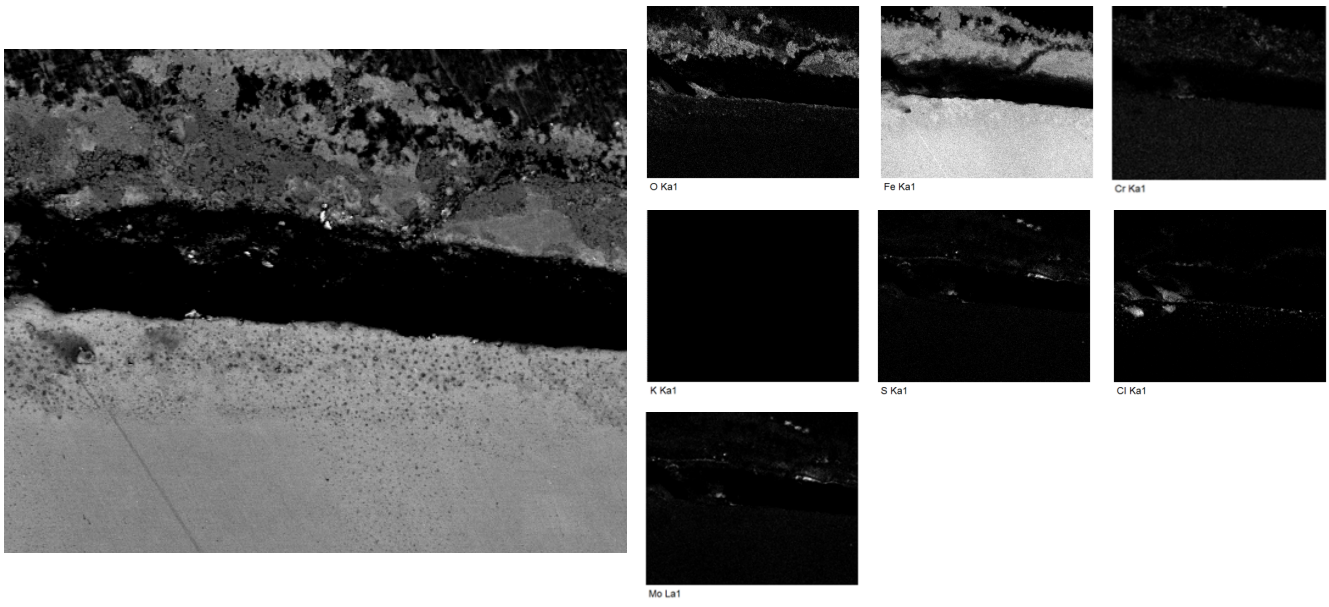

Figure 35: EDX analysis of the flue gas side of 13CrMo4-5 Ref Ref at 525 °C for 2000h.

- Corrosion memory 13CrMo4-5: waste + SR 1000h - waste 1000h at 525 °C (Rec Ref)

Regarding the corrosion memory samples. The 13CrMo4-5 Ref Rec (1000h in reference line first + 1000h Sulfur Recirculation line) and 13CrMo4-5 Rec Ref (1000h in Sulfur Recirculation line first + 1000h in reference line) show respectively an average material loss of 322 and 350 µm. All 13CrMo4-5 samples exposed in the line with sulfur show a lower average material loss than the sample exposed only in the line without sulfur.

The **Figure 36** shows the backscattered images of the 13CrMo4-5 Rec Ref sample. Both sides have oxides on top of the material of ~390 µm on the shadow side and a total thickness of ~650 µm on the flue gas side. The flue gas side has a higher material loss which agrees with the Figure 19.

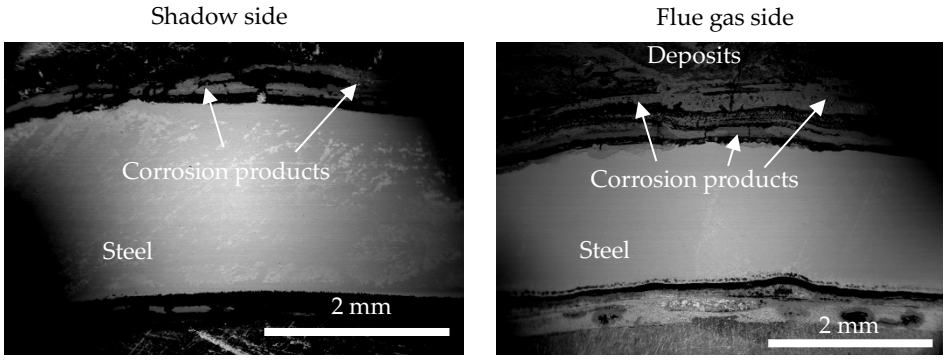

Figure 36: BSE image showing a low mag cross section of 13CrMo4-5 Rec Ref at 525 °C for 2000h.

The EDX analysis represented in **Figure 37** shows that the oxide scale is formed by multiple oxide layers mainly constituted of iron oxide. Sulfur and chlorine were detected only at the interface metal oxide. No potassium detected.

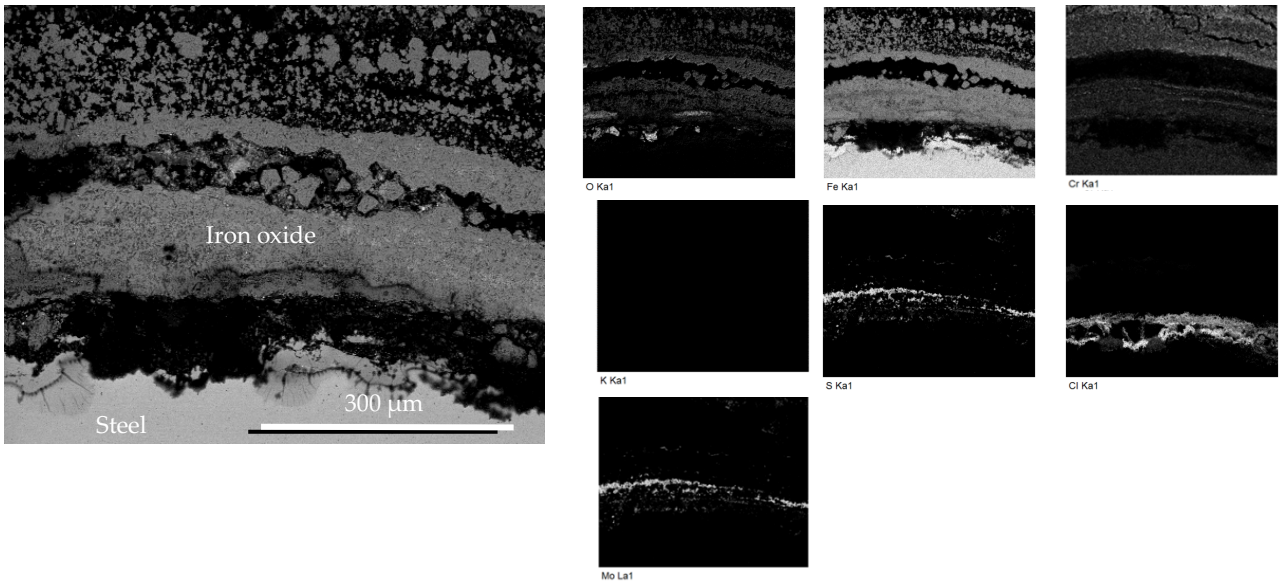

Figure 37: EDX analysis of the flue gas side of 347 Rec Ref at 525 °C for 2000h.

- Corrosion memory 13Cr: waste 1000h – waste + SR 1000h at 525 °C (Ref Rec)

The **Figure 38: BSE image showing a low mag cross section of 13Cr Ref Rec at 525 °C for 2000h.** shows the backscattered images of the 13Cr Ref Rec. The deposits fall off on both sides. On the shadow side, the surface looks smoother than the flue gas side. Corrosion products can be observed on both sides.

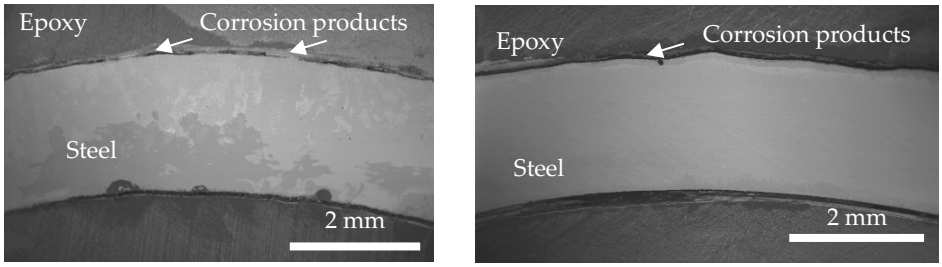

Figure 38: BSE image showing a low mag cross section of 13Cr Ref Rec at 525 °C for 2000h.

The EDX analysis represented in **Figure 39** shows a layer of inward growing spinel oxide on top of the material. A great amount of chlorine, as well as traces of sulfur can be observed within the iron oxide layer. No potassium detected.

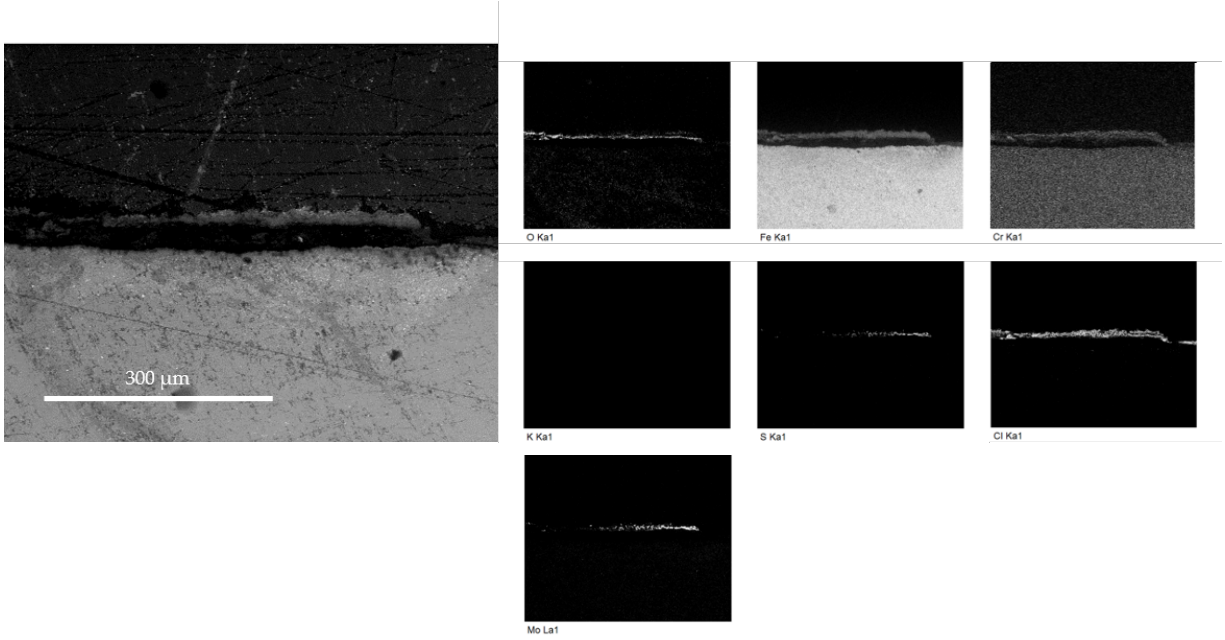

Figure 39: EDX analysis of the flue gas side of 347 Ref Rec at 525 °C for 2000h.

5.1.5 Corrosion in the superheater region - fixed installed superheaters

In order to measure the corrosion rate in the same conditions as the full scale superheaters, different material samples were welded into the actual superheaters

as described in section 3.1.3 and extracted after ½ and 1 year of operation respectively. The corrosion rate of the fixed installed superheater test materials in mm/year was measured by an ultrasonic thickness gauge at 4 different positions per ring: wind, lee and both sides. The standard deviation of the initial thickness measurements was in the range of 0.1 mm, the measured corrosion rates varied substantially between different rings, even at the same position. Therefore, mean values were formed for all rings, grouped by material type in **Figure 17**: Low alloyed corresponds to 16Mo3 and 13CrMo4-5; stainless steels to TP347H and W1.4841 (314); High alloyed to Sanicro 28 and 3RE28 (310). The low alloyed mean corrosion rate was some 50% lower and max some 40% lower in the Sulfur Recirculation line. However, since the corrosion rates have historically been higher in that line, the effect of Sulfur Recirculation is probably higher. The stainless steels mean corrosion rate was almost 80% lower, while the max values were approximately 35% lower. It was difficult to draw any conclusion from the high alloyed materials since the corrosion was in the order of the standard deviation of the initial thickness, which is reflected by the large number of measurements with apparent material growth.

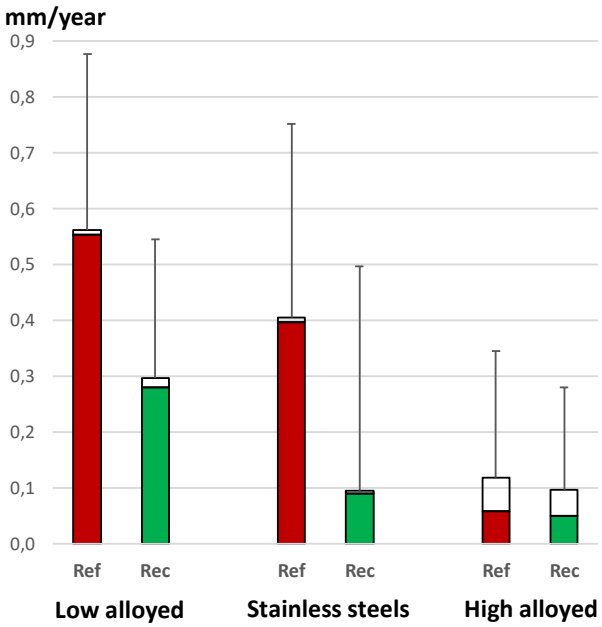

Figure 40 The filled bars denote the mean corrosion rate of fixed installed superheater test materials in mm/years. The entire bars denote the corrosion rate when all measurements with apparent material growth was discarded. The top error bar reading denotes the mean value of the max corrosion rate per ring.

5.1.6 Corrosion in the full-scale superheaters

The corrosion rate in the actual superheaters is measured periodically, twice per year, by Babcock & Wilcox Vølund A/S in order to assess and plan maintenance need and super heater exchange which has previously been done approximately every 3 years. The results from the Sulfur Recirculation line is shown in Figure 41. The numbers are comparable to the low alloyed superheater test material results in Figure 40.

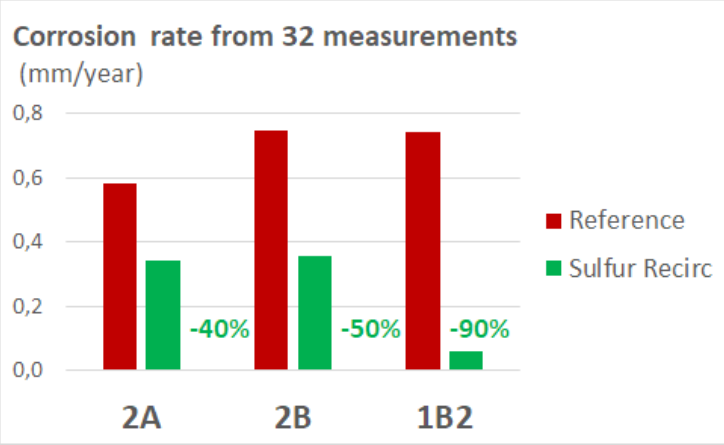

Figure 41 Mean corrosion rates in the actual superheaters for 1 year prior to Sulfur Recirculation operation (here denoted Reference) and 1 year of operation with Sulfur Recirculation in the same boiler.

5.2 CORROSION MEMORY/MICROSTRUCTURE - LABORATORY EXPOSURES

A more detailed description of the results from the modified 310 steel and the TP347H steel are given in appendices.

5.2.1 Exposures with modified 310 steel (heat-treated vs as received)

Pre-exposure assessment of the microstructure of the modified 310 steel heat-treated (700ºC for 10000 hours) was compared with the as received. No sigma phase was visible in the as received and there was 29 vol. % sigma phase in the heat treated specimen (Figure 42). Furthermore, it was confirmed by long term isothermal heat treatments that sigma will not form to a large extent at the test temperature (600 ˚C) for the duration of the test (168h).

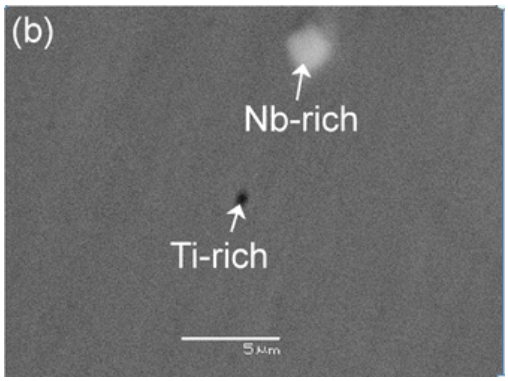

As received

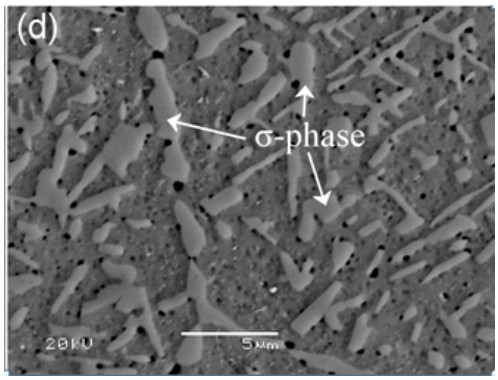

Heat treated

Figure 42: Comparison of pre-exposed microstructure

The presence of phases in the modified steel is calculated with ThermoCalc showing that sigma phase is stable in the temperature area. TEM analysis reveals sigma phase and its composition (Figure 43) for the heat-treated steel.

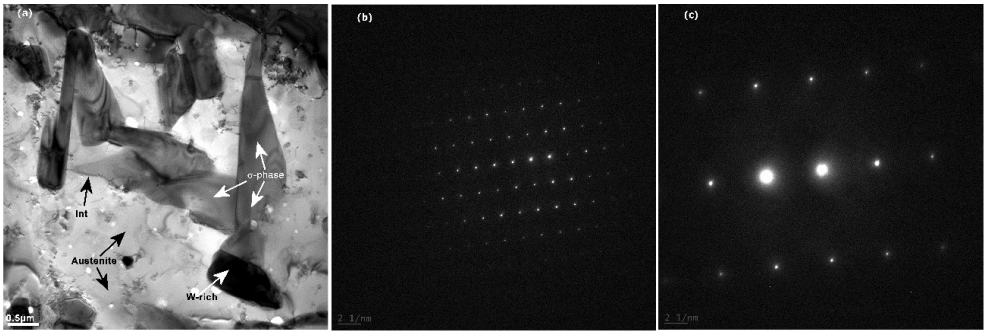

a) TEM image **b) diffraction from σ phase** **c) diffraction from austenite**

Composition (Wt. %)	Cr	Fe	V	Mn	Ni	Nb	W
TEM: Austenite	21.3	52.1	0.4	1.1	25.2	-	-
TEM: σ-phase	43.8	38.8	0.3	0.6	7.5	-	9.1

Figure 43: TEM results, diffraction patterns and EDX analysis of the heat-treated modified 310

Figure 44 shows RLM images of the corrosion tested steel in both as received and heat-treated condition, exposed both with and without the presence of KCl. Selective internal corrosion was observed for the heat-treated sample in both KCl-free and KCl-bearing exposures. In the KCl-free exposure, the heat-treated sample showed an increased corrosion attack compared to the as received sample. However, in the presence of KCl a drastic increase in corrosion attack was observed for the heat-treated sample both compared to the reference exposure and compared to the as received sample exposed in the presence of KCl.

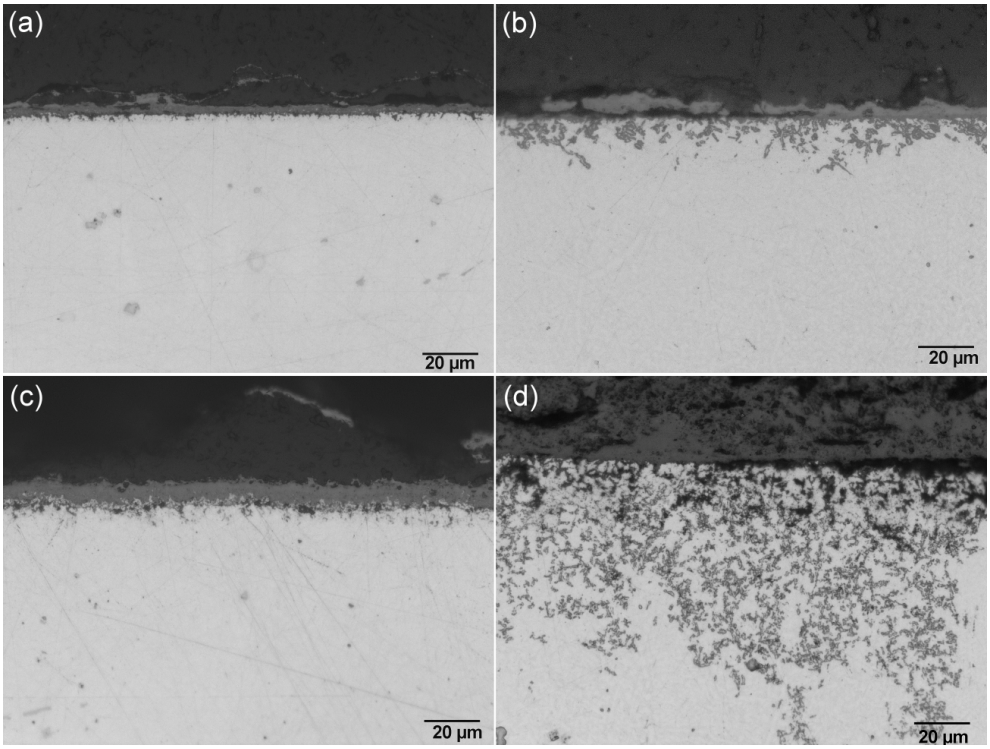

Figure 44. RLM micrographs after exposure in a 15 % (v/v) H_2O (g) + 5 %(v/v) O_2 (g) + N_2 (g) (balance) atmosphere at 600°C for 168h. (a) as received KCl-free sample (b) heat-treated KCl-free sample (c) as received covered with KCl sample (d) heat-treated covered with KCl sample

The SEM micrographs in Figure 45 show that the outer oxide is iron rich and the inner darker oxide is chromium rich. In addition, the areas in the middle of the internal attacked zone and at the corrosion front are similar. In both cases the preferential attack is at or around the sigma phase. From EDX analysis, there is no Cl in the matrix, however Cl can be found at areas where there was previously sigma phase. In addition, Cl was detected in substantial quantities at the corrosion front

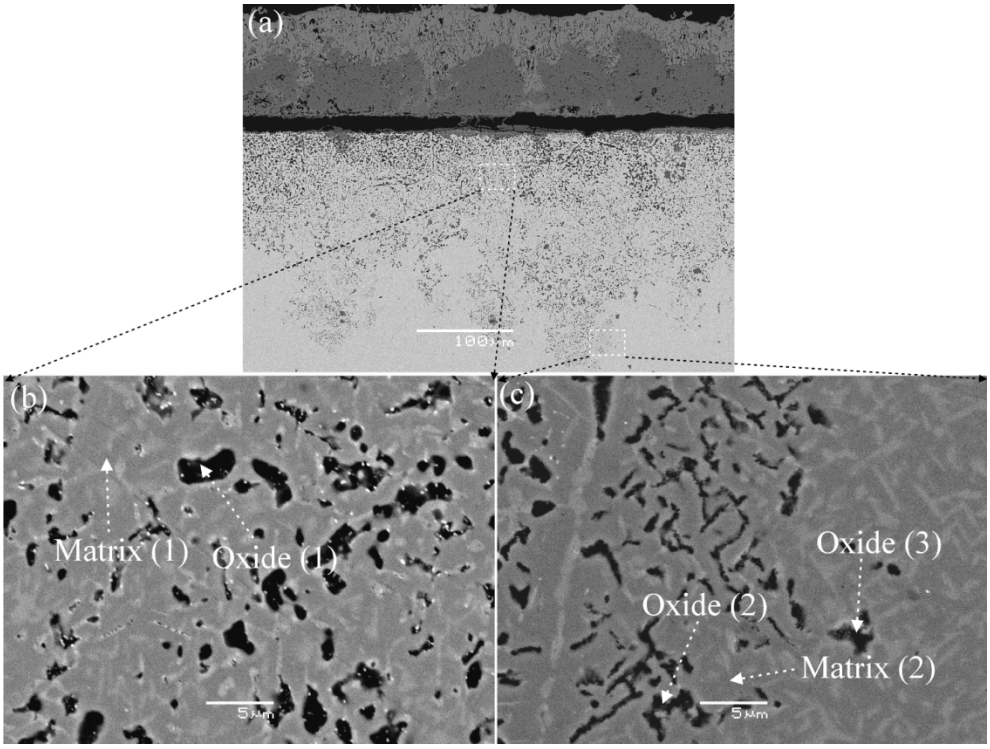

Composition (Wt. %)	O	Cl	K	Cr	Fe	Ni	Cu	W
Matrix (1)	-	-	-	17.9	50.9	31.2	-	-
Oxide (1)	21.0	7.6	1.1	7.0	30.7	23.4	3.3	6.0
Matrix (2)	-	-	-	20.1	51.9	24.8	3.2	-
Oxide (2)	11.8	2.3	-	16.2	38.5	18.8	2.3	10.0
Oxide (3)	4.77	8.0	-	17.6	40.8	18.4	3.2	7.2

Figure 45. RLM micrographs after exposure in a 15 % (v/v) H_2O (g) + 5 %(v/v) O_2 (g) + N_2 (g) (balance) atmosphere at 600°C for 168h. (a) as received KCl-free sample (b) heat-treated KCl-free sample (c) as received covered with KCl sample (d) heat-treated covered with KCl sample

Transmission electron microscopy (see appendix) at the corrosion front shows voids which could be due to oxides removed during thinning. Cl was present within the

oxide areas, and the oxide was observed to contain less Cr than the matrix, and also a chromium depletion zone close to the oxide could be observed.

XRD analysis (see appendix) was conducted both on the modified 310 steel as received and after various heat treatments, and after corrosion exposure. For the pre-exposure steels, there was no sigma phase in the as received but clearly sigma phase in the steel heat-treated at 700ºC for 10,000 hours. After the corrosion exposure, the outer corrosion product was removed by polishing, and XRD revealed in addition to austenite, hematite and magnetite phases, but no indication of sigma phase.

5.2.2 Exposures with 347H, aged vs as received

The microstructures of 347H FG steel in as received and aged condition (plant exposure) after etching is shown in Figure 46 where the as received sample revealed few precipitates as shown in Figure 46a. A relatively higher amount of precipitates with morphology typical of σ-phase could be found in the 0º aged sample than the 180º aged sample, cf. Figure 46c and Figure 46b. The precipitates are mainly located at grain boundaries and triple junctions.

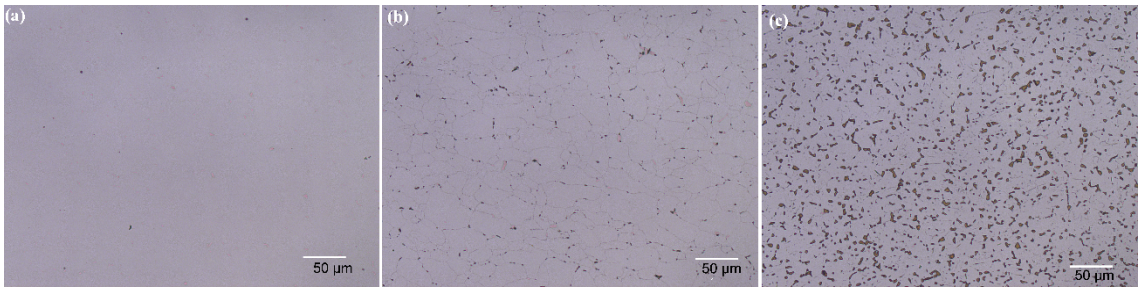

Figure 46. LOM micrograph of a) as received, b) aged (180º from flue gas), c) aged in flue gas direction (0 º). The samples are etched electrolytically with 10% KOH in water

The as received sample showed less corrosion attack and less significant grain boundary attack as compared to the aged samples (Figure 47). The SEM-EDX analysis of the as received sample revealed an outer Fe-rich oxide and an inner Fe-Cr-Ni oxide.

The 180º and 0º aged samples, at the middle of the specimens, showed similar kinds of microconstituents: an Fe-rich outer oxide layer, an inner Fe-Cr-Ni oxide, and grain boundary attack. Nevertheless, the severity of attack was higher in the 0º aged sample. Occasionally, regions associated with K-Cr-O were found, for example in Figure 47b.

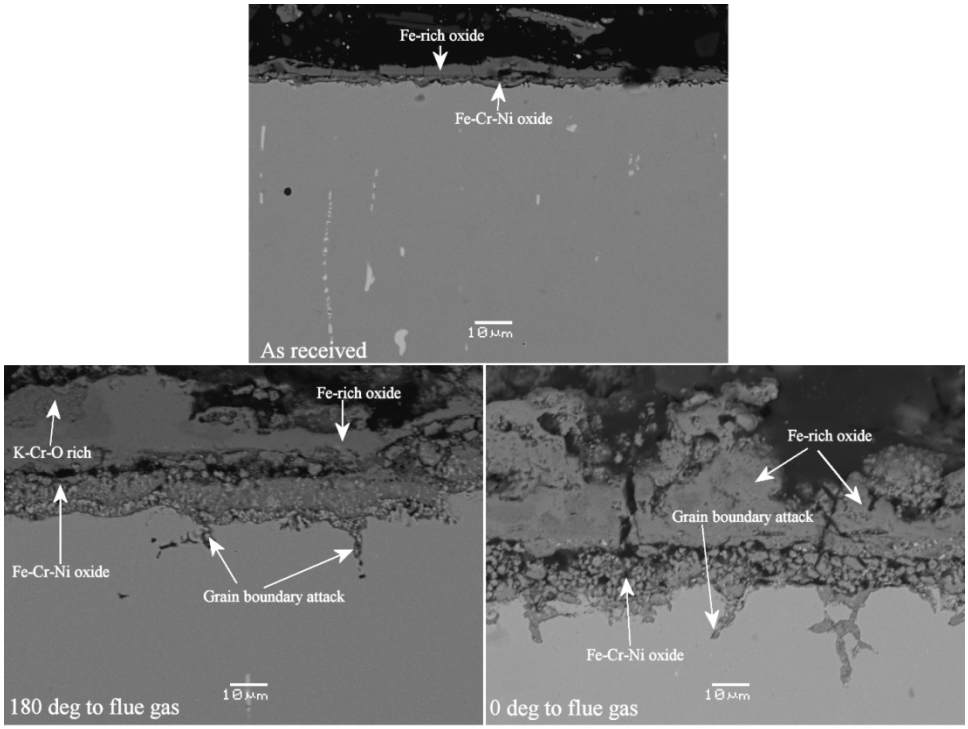

Figure 47. Back scattered images of a) as-received, b) aged sample 180º from flue gas direction and c) aged sample in the flue gas direction (0 º) after covering with KCl and exposing in 5 % (v/v) O_2 (g) +15 % (v/v) H_2O (g) + N_2 (g) (balance) atmosphere at 600˚C for 168h

Similar to the 180◦ aged sample, Cr-rich σ-phase is present ahead of the oxide at the corrosion front of the 0º aged sample (Figure 48). Unattacked discontinuous σ-phase was also observed from this sample. This suggests that not only the presence of σ-phase but also the connectivity among σ-phases is important to accelerate the corrosion rate.

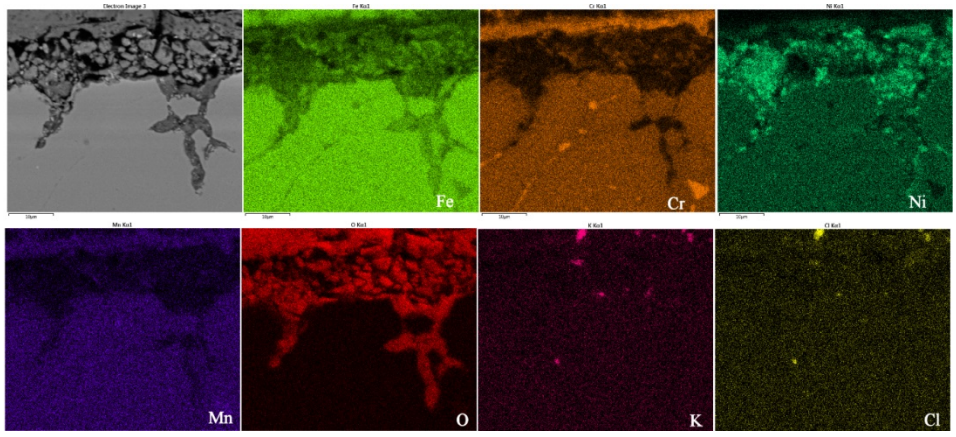

Figure 48. Back scattered SEM image of the 0º aged sample covered with KCl after corrosion exposure in 5 % (v/v) O2 (g) +15 % (v/v) H2O (g) + N2 (g) (balance) atmosphere at 600˚C for 168h

To get an idea about the initiation reactions of accelerated corrosion in KCl bearing environment, plan view analyses was performed as a complement to the cross-section investigations. The plan view of 0º aged sample is presented with the corresponding XRD analysis (Figure 49). The outer oxide was mainly composed of

porous Fe-rich oxide and K-Cr-O rich particles. In regions where spallation occurred, Fe-Cr rich and some Ni oxide was also found. The XRD result confirmed the corresponding phases as Fe-rich M_2O_3, K_2CrO_4 and Fe-Cr-Ni spinel (M_3O_4).

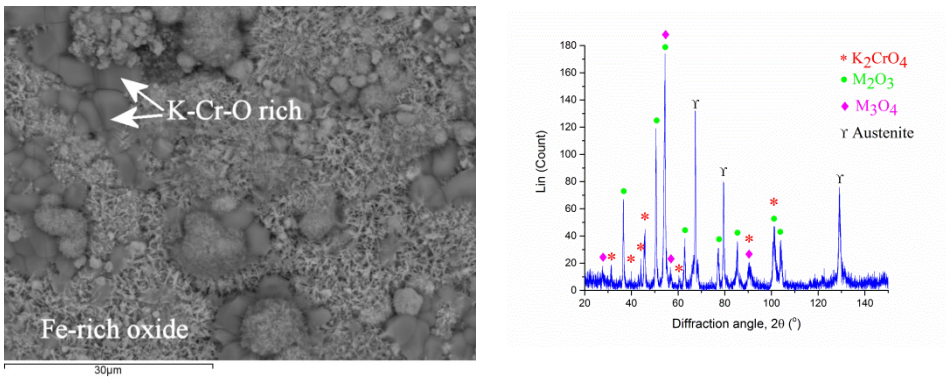

Figure 49. a) Top view of aged sample in the flue gas direction (0 º) covered with KCl and exposed 5 % (v/v) O2 (g) +15 % (v/v) H2O (g) + N2 (g) (balance) atmosphere and b) corresponding XRD analysis

5.3 CORROSION MEMORY/MICROSTRUCTURE - FIELD EXPOSURES

5.3.1 Comparison of different environments for Esshete 1250

In this section, Esshete 1250 specimens from different plants are compared with respect to fireside corrosion and the microstructure evolution at the corrosion front. Further details are given in the Appendix. Figure 50 shows the corrosion front from boiler A where the inner corrosion product is chromium rich oxide and sulfur can also be found close to the metal interface. The alloy below the oxide consists of a Cr depleted layer especially in grain boundaries and S is present in the dark corrosion product together with Mn, as Esshete 1250 contains 6 wt.% Mn. At the area below the sulfides, there is Cr and Mn depletion at grain boundaries, resulting in Fe and Ni enrichment (green analysis). The dark precipitates present below this area at the grain boundaries are Cr rich (red analysis) whilst the light precipitates are Nb or Mo rich. Generally, the larger particles are Nb rich whilst the small particles are Mo rich. The red arrow indicates the direction of the fireside surface. The dark Cr rich precipitates in the microstructure are apparent on the fireside part of the tube, and their presence decreases from the fireside surface of the tube

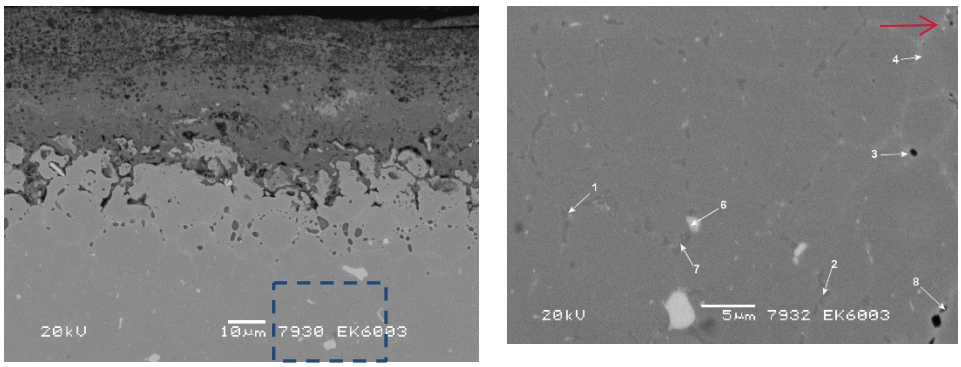

F-7932	Si	S	V	Cr	Mn	Fe	Ni	Nb	Mo
1	0.6			16.1	6.7	66.3	9.3		0.9
2	0.3	0.7	0.8	49.0	4.7	33.6	5.4		5.4
3	1.1	0.7		8.1	2.3	68.0	18.0		1.8
4	2.2		0.6	11.5	2.7	58.1	18.7	1.0	5.4
6			0.4	6.2	2.3	21.4	2.4	67.2	
7	0.3	0.2	0.6	39.5	5.4	43.1	5.4		5.6
8	0.6	4.0		5.1	4.0	66.7	19.6		

Figure 50: Fireside oxide for Esshete 1250 from boiler A and analysis of precipitates below corrosion front

The fireside oxide from the specimen from plant B had some similarities to plant A. Cr rich precipitates were present within the alloy below the sulfidation rich zone, and Cr depletion at the grain boundaries was immediately above this (*Figure* ***51***). This was not observed on the steamside.

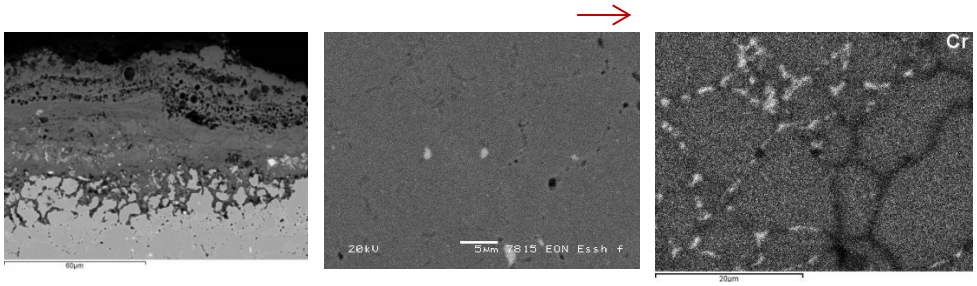

a) Fireside oxide *b) below corrosion front* *c) Cr mapping for Fig 5b*

Figure 51: Morphology of fireside oxide on specimen B (co-firing) and Cr mapping below the corrosion front

The fireside oxide from boiler C only revealed localised grain boundary attack and the presence of Cr rich precipitates was not apparent with SEM. In comparison to the specimen from boiler B, this specimen has had a longer exposure at slightly lower temperatures.

For boiler D, a biomass boiler at much lower temperatures, in some areas there was a thick oxide layer and preferential attack at the corrosion front (Figure 52) but grain boundary attack was not so deep compared to specimens A and B, but is present around the total circumference. In some areas, a darker phase at grain boundaries was just visible but could not be clearly identified as Cr rich, however if it was very thin, the interaction volume of the analysis would not give a reliable result. At the corrosion front, there was Cr depletion and the Cr rich corrosion product was just below the area of Cr depletion.

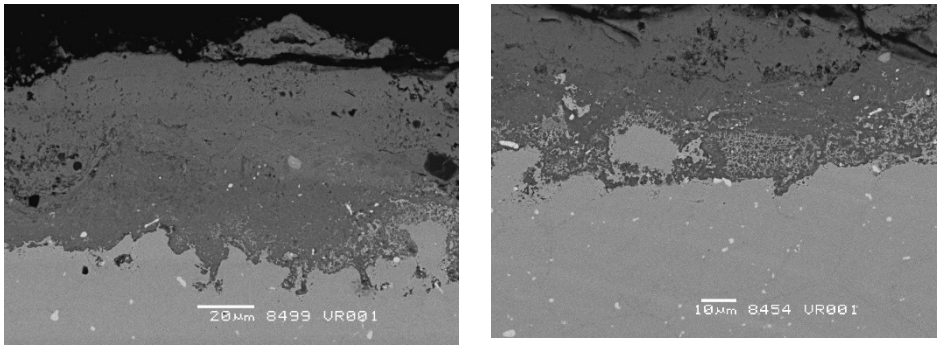

Figure 52: Morphology of fireside oxide on Specimen D

5.3.2 Comparison of different materials:

A comparison on the exposed specimens at boilers E and F are given in Figure 53.

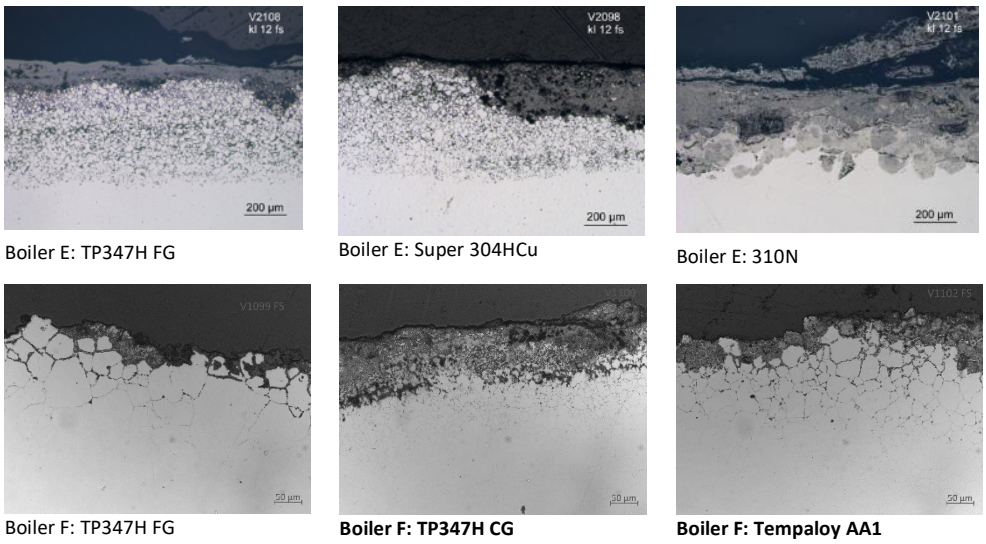

Boiler E: TP347H FG | Boiler E: Super 304HCu | Boiler E: 310N

Boiler F: TP347H FG | **Boiler F: TP347H CG** | **Boiler F: Tempaloy AA1**

Figure 53: Comparison of attack for tubes exposed in boiler E and F

It is clear from Figure 53 that there is internal attack at the corrosion front for all the steels investigated. Scanning electron microscopy reveals Cr depletion at the corrosion front and as was clear from light optical microscopy, preferential attack at grain boundaries, especially for the 18% Cr steels (Figure 54).

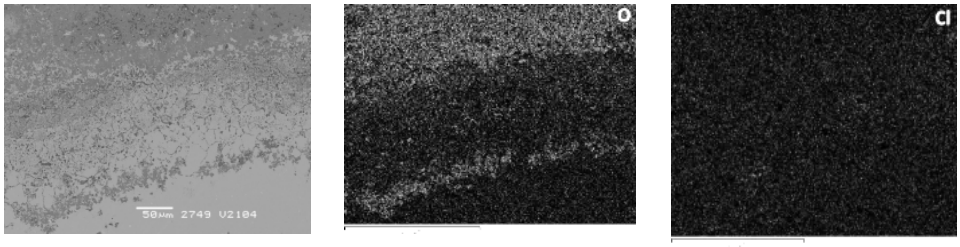

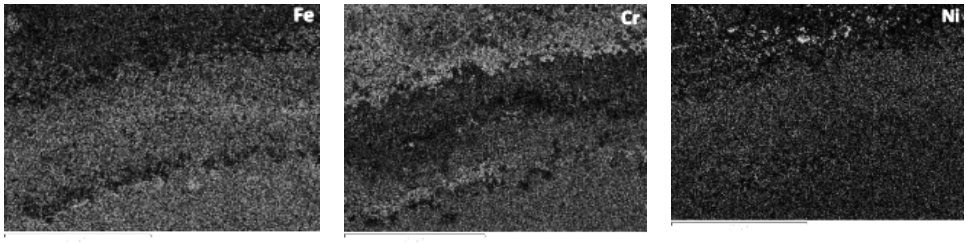

Figure 54: Scanning electron microscopy of corrosion front for Super 304 exposed in boiler E

Figure 55 shows the corrosion front where both traces of Cl and traces of S are sometimes analyzed in localized areas which are seen as pores in the micrograph. In addition, precipitates are sometimes observed for this specimen in the microstructure adjacent the corrosion front. Figure 17b shows the microstructure adjacent the corrosion front in boiler C after 101,100 exposures where this zone with precipitates was wider and was always present.

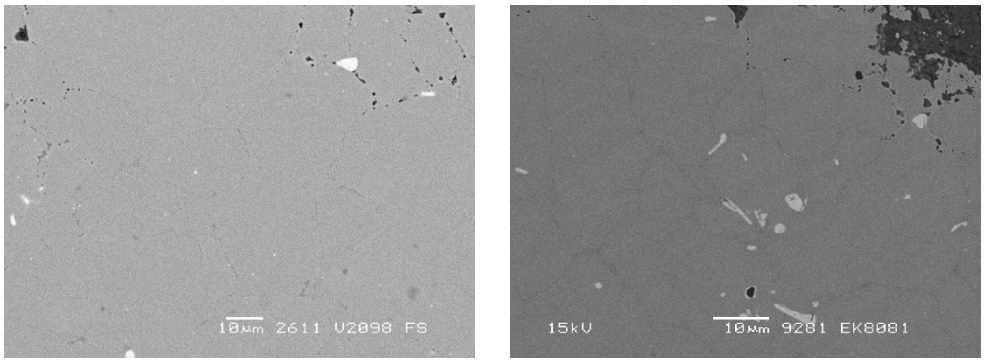

Figure 55: Scanning electron microscopy of corrosion front of a) Super 304 exposed in boiler E, and b) TP347H FG in boiler C after 101100 hours

Different etchants and times were used to try and reveal the underlying microstructure at the corrosion front. For this purpose, the tube with a penthouse section and a combustion area section is compared from Boiler F (Figure 11). There is clearly a different response for the two specimens, although they are from identical steel batches and have had the same exposure time Figure 56.

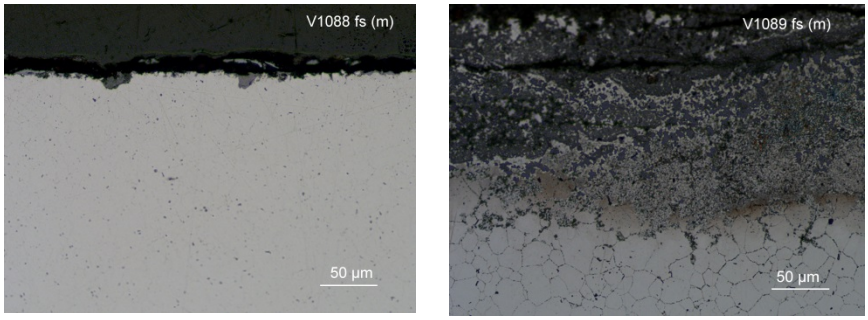

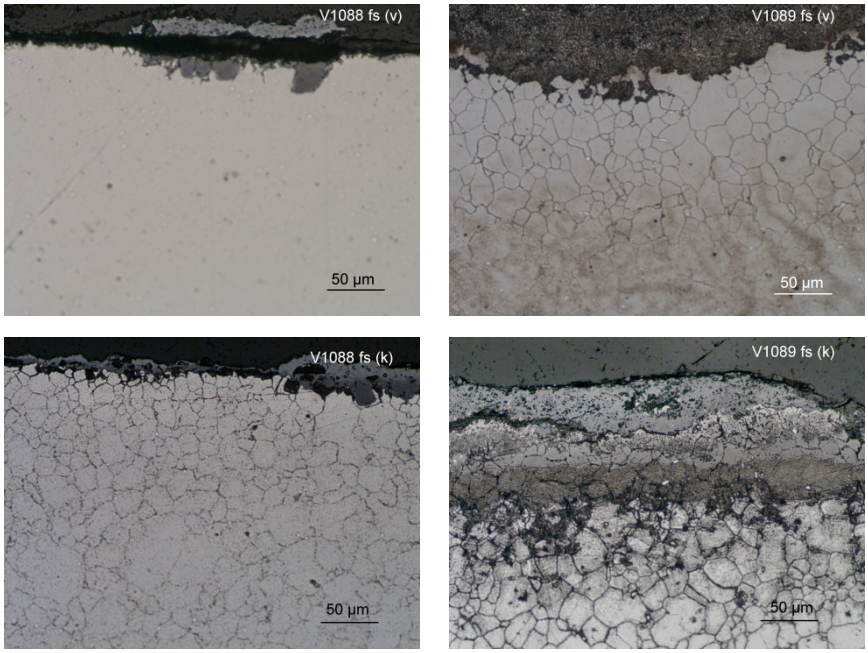

Figure 56: Use of etchants revealing microstructure 347H from penthouse and within the boiler. the lefthand side is from the penthouse and the right-hand side from within the boiler

The etched specimens were investigated with SEM, however in many cases it was clear that if there had been something at the grain boundaries, this had been removed by the etching process. So, although etching reveals some changes in the microstructure due to fireside corrosion, care has to be taken with respect to the analysis method as to how to characterize the extent and nature of this change in microstructure.

Due to the broad zone of precipitates adjacent the corrosion zone shown in Figure 55b, this specimen was used to find a method to analyse the precipitates. On a small section of the convex fireside, the oxide was removed until the metallic surface could be observed. This was analysed with XRD, and only peaks for austenite were observed. On another section, the specimen was mounted and ground and polished to remove surface deformation and after a very light etch to reveal grain boundaries, a FIB lift-out across a grain boundary was taken close to the corrosion front (Figure 57). TEM analysis of this FIB lift-out revealed large Cr rich $M_{23}C_6$ precipitates on the grain boundaries. In addition, fine $M_{23}C_6$ precipitates was observed in the grains where they were more prevalent close to grain boundaries.

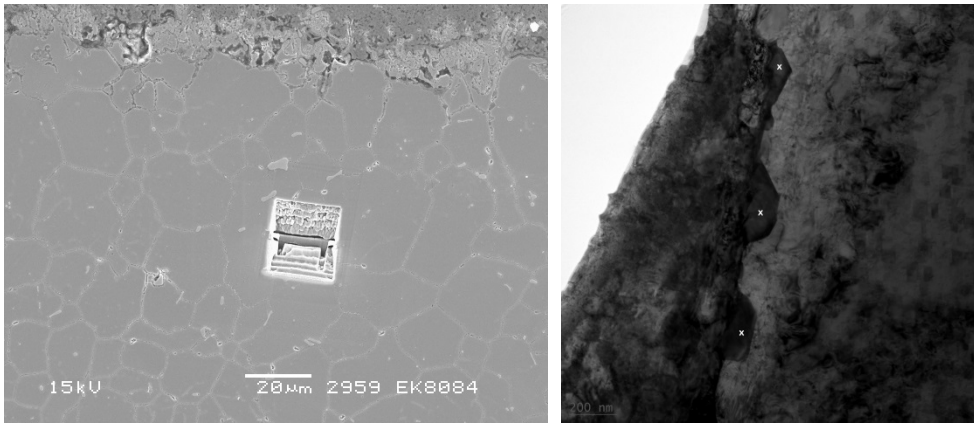

Figure 57: Position where FIB was taken from fireside, and TEM micrograph showing precipitates on grain boundary. The specimen is from 347H from boiler C exposed for 101100 h

6 Analysis of the results

The fuel selection has a large impact on the operation of a CHP plant. Cheaper fuels are normally more corrosive which may result in increased maintenance costs, due to corrosion. In order to keep the corrosion under control the steam parameters are usually lowered resulting in not only lower corrosion rates but also a drop in electrical efficiency. Thus, the green electricity production from these corrosive fuels are directly dependent on more effective corrosion mitigation techniques are needed. The Sulfur Recirculation technique has previously in short term test indicated that it may be one possible solution to decrease the corrosion rates in waste fired CHP plants. In connection to this project the impact of the technique has been studied at the first full scale commercial installation in MEC Denmark. The results are well in line with the preliminary indications, i.e. the Sulfur Recirculation technique decreases the corrosion of the superheaters through a change in chemistry of the formed deposits.

The fuel selection for the CHP plants may in addition change over time, i.e. there may be a need to optimize and correlate the boiler operation to current fuel quality. A potential limiting factor in this type of operation is periods of accelerated corrosion, severely decreasing the lifetime of e.g. the superheaters in the boiler. However, little is known about how the corrosiveness varies over time with variations in the fuel mix. How much of the current corrosion attack is due to the corrosion history (i.e. previous deposit build-up and oxide scale formation) rather than the current flue gas composition (i.e. current fuel mix being used)? The first commercial full-scale installation at MEC has in this work provided an excellent platform in order to study the environmental corrosion memory effect with the two parallel lines representing different corrosive fuel. The other aspect of corrosion memory is related to the bulk material. How will long term changes in alloy microstructure and composition influence the high temperature corrosion resistance? The corrosion memory effect can thus be divided into two aspects, i.e. environment and material.

The present project aims to increase the knowledge of the long-time effects of the Sulfur Recirculation techniques as well as materials technology process solutions to minimize superheater corrosion with advanced steam data in boilers. The obtained results will contribute to the understanding of how a power plant with advanced steam data can be operated with variations in fuel quality. By generating long term knowledge about the Sulfur Recirculation and addressing the corrosion memory effect, boiler operators will benefit by getting tools to minimize the corrosion using smart operational strategies.

The project consists of three parts, i.e. the Sulfur Recirculation and the influence on the corrosion of the superheaters as well as the two aspects of corrosion memory. Thus, increasing the knowledge in one of the two corrosion memory sub-areas described above; namely the rate of conversion of corrosive deposits.

The ambition has been to be able to answer the following questions:

- Investigate the long-time influence on the corrosion of the full-scale installation of the Sulfur Recirculation technique in MEC.
- Investigate the corrosion memory effect – environment. Could a remaining effect be found from deposit formed in a corrosive/less corrosive fuels?
- Investigate the corrosion memory effect – material. Could long term changes in microstructure and composition of an alloy influence its high temperature corrosion resistance?

6.1 SULFUR RECIRCULATION

Sulfur Recirculation was successfully operated during the experimental time period and onwards. Due to the increased sulfation of the fly ash, almost all of the sulfur entering with the fuel ended up in the fly ash, almost eliminating the need for transporting sulphate water away by truck. The HCl produced from sulfating alkali chlorides is small compared to the HCl concentration already present in the flue gas [1].

The corrosion study was focused on the stainless steel 347H and low alloyed 13CrMo4-5. In both cases there is an effect of the changed environment and a higher level of sulfur produces a less corrosive deposit. Sulfur Recirculation shows a positive effect on both the 347H and 13CrMo4-5 materials corrosion rates already during the relatively short corrosion probe exposure times.

The stainless steel 347H probe exposures show a difference in material loss between the reference line and the Sulfur Recirculation line, shown Figure 18. The sample exposed in the reference line (waste) during 2000h presents a 0,05 mm material loss compared with the negligible material loss of the sample exposed 2000h in the Sulfur Recirculation line. The stainless-steel samples in the fixed superheater installation showed an 80% decrease in mean corrosion rate and 35% decrease in max corrosion rate (Figure 40).

In the case of the low alloyed steel 13CrMo4-5 corrosion probe samples, material loss can be observed on all samples at 525 °C as this is a high material temperature for a low alloyed steel. The reference sample (2000h in the waste line) shows the highest material loss while the Sulfur Recirculation sample (2000h in the Sulfur Recirculation line) shows the lowest value. This demonstrates that the sulfur has also a positive effect on the 13CrMo4-5. The low alloyed mean corrosion rate was some 50% lower and max some 40% lower in the Sulfur Recirculation line for the fixed superheater test samples (Figure 40). The actual superheater mean corrosion rate decreased by some 40-90% when comparing to the previous operating year as seen in Figure 41.

In the case of the air-cooled probes, the both highly alloyed Sanicro 28 and 310 samples show very little or no measurable material loss in all the different conditions (**Figure 18**). It is therefore not possible to draw any conclusions regarding the effect of sulfur on their corrosion resistance.

The full-scale Sulfur Recirculation technique installed in the CHP plant MEC changes the deposit chemistry, and less corrosive species end up on the

superheaters. This results in less corrosion of the superheaters both on low alloyed steels and on stainless steels. Thus, the results are well in line with the preliminary indications, i.e. the Sulfur Recirculation technique decreases the corrosion of the superheaters through a change in chemistry of the formed deposits. The effect of sulfur has previously been studied from a corrosion perspective. Four different mechanisms have been identified:

- Transforming alkali chlorides to alkali sulfates gives less reactive alkali on the superheater breaking down the Cr rich protective scale (stainless steels)[8]
- Transforming alkali chlorides to alkali sulfates gives less Cl on the superheaters (both low alloyed and stainless steels) [8]
- Iron oxide grows slower in the presence of small amounts of SO_2 (low alloyed steels or stainless steels after breakaway oxidation) [18]
- Formation of iron sulfide at the metal/oxide interface may increase spallation of the oxide scale [18]

The results are well in line with three of the proposed mechanisms and the largest impact could be observed on the stainless steels where all three mechanisms are expected to be at play. However, no increased tendency for spallation in the presence of an increased SO_2 level could be identified during the exposures and no increased levels of metal sulphides could be identified during the microstructural investigation.

6.2 CORROSION MEMORY – ENVIRONMENT

Within the corrosion memory – environment study of this project an extensive air-cooled deposit/probe campaign have successfully been performed in the commercial CHP plant MEC. The exposure campaign was divided into a short-term exposure (24h + 24h) and a long-term exposure (1000h + 1000h). Four different air-cooled probes were used simultaneous in order to be able to investigate the memory effect. The set-up of the two lines at MEC offered the possibility to switch probes with a very limited drop in temperature. The aim was to run the exposures at two temperatures in order to investigate if the temperature has an effect on the memory effect. The selected temperatures (different zones on the probes) were 400 °C as it represents the current material temperature of superheaters and 600 °C in order to accelerate the test to be able to reveal differences after the exposures. However, the flue gas temperature did not allow a higher material temperature than 525 °C at the position where it was possible to insert the air-cooled probes. Commercial representative alloys were selected for the investigation. The alloys represent low alloyed steels (13CrMo4-5), stainless steels (347H) as well as highly alloyed stainless steels (San28 and 310). An exposure temperature of 525 °C limits the possibility to investigate the highly alloyed steel as the corrosion rates are very low during the duration of the exposures. The 13CrMo4-5 represents the material class of iron oxide forming alloys despite the low amount of Cr in the alloy. It has previously been shown that the alloy has a similar oxidation behaviour but the low amount of Cr may act as a marker to separate inward and outward growing scales.

6.2.1 Initial deposit formation

The aim with the short-term exposures was to investigate the kinetics and temperature dependence of the reactions of two deposits formed in the two different boilers (environments), i.e. the environmental memory effect. The exposure scheme gave 32 samples where the two reference samples (Rec Rec and Ref Ref) represents the deposits formed under normal conditions in representative environment. Two memory effects were investigated, i.e. a first period of more corrosive fuel followed by a less corrosive fuel (Ref Rec) and the other way around (Rec Ref).

The recirculation line has a slightly higher concentration of sulfur than the reference line, and this observation meet the expectations as the reference line does not have any sulfur added (Figure 15). Regarding the chlorine concentration, Figure 14 shows that the recirculation line has a lower value (0,75%) than the reference line (1,09%). However, the memory effect probe Rec Ref exhibits an even higher value of chlorine than the two previous ones while showing also a higher value in sulfur content. This is an interesting observation as less chlorine is expected when sulfur is present and may be an effect of temporary variation in the flue gas during the very short exposure.

6.2.2 Propagation – deposit formation and corrosion attack

The second set of exposures lasted for 1000h + 1000h in order to study the propagation stage and the memory effect of the different environments. Regarding the IC results for 2000h, for the chloride content, both the corrosion probe deposits and the superheater deposits from the recirculation line exhibit a significant reduction of chloride concentration as expected (Table 13). Thus, the recirculation of sulfur reduces the amount of chloride found in the deposits.

The recirculation line shows a higher value of sulfur and a lower value of chloride than the reference line. These observations are expected and may act as the two cases where the memory effect samples should be compared to. Regarding the corrosion memory probes, there were a large spread in the results. The dense hard deposits made it very difficult to remove a representative part of the deposit. As a result, this may only reflect some of the deposits. Therefore, it is not possible to draw conclusions regarding a memory effect on the deposits composition during 2000h and the effect could instead be studied through the corrosion attack.

In the case of 347H, the sample exposed 1000h in the Sulfur Recirculation line (first) and 1000h in the reference line (after), presents a considerable less material loss (0,03 mm) than the one exposed only in the reference line, but more than the one exposed in the Sulfur Recirculation line (Figure 19). This indicates a positive corrosion memory effect of the sulfur rich environment/deposit for the 347H material. In line with these results the sample exposed first 1000h in the reference line and 1000h in the Sulfur Recirculation line showed a higher material loss than the reference sample indicating a corrosion memory effect also in this case. The results of the stainless-steel shows indications about different corrosion memory effects depending on which order the fuels/flue gas/deposits forms. The positive memory effect which is translated by a mitigation of corrosion, is given when the less corrosive fuel comes prior to the less corrosive fuel.

For 13CrMo4-5 samples, is it possible to observe indications of memory effects even though the material temperature is high for this type of material. As mentioned previously, the reference sample (2000h in the waste line) presents the highest material loss of all of them while the Sulfur Recirculation sample (2000h in the Sulfur Recirculation line) shows the lowest value. The corrosion memory samples (1000h in each line) present intermediate values in both cases (**Figure 18**).

The 347H and 13CrMo4-5 were selected for a further material loss profiling and microstructural investigation by SEM/EDX. In the case of the 347H material, the corrosion attack is mainly located to the flue gas side. The cross section reveals indications of a steel grain boundaries attack. The chemical analysis shows the presence of metal chlorides located at the interface metal/oxide in all cases (**Figure 23Figure 25** and**Figure 31**), except in the Rec Ref case where less chlorides are present (**Figure 28**). No protective chromium layer could be observed on any of the investigated 347H indicating that alkali reacted with the Cr rich oxide on an early stage. The inward growing spinel oxide is expected to be formed as it is observed in the Rec Ref case (**Figure 28**) where an oxide thickness of ~ 50 µm could be observed. While in the other cases, the determination of oxide thickness was not possible due to spallation during exposures or sample handling.

The low alloyed steel 13CrMo4-5 is in overall more corroded than the 347H as expected. The flue gas side shows again signs of higher corrosion rates than the shadow side, which agrees with the material loss in Figure 19). As expected, the 13CrMo4-5 is more corroded in the Ref Ref environment than in the Rec Rec case. Almost all cases exhibit a broken layer of iron oxide thicker than the one observed in the 347H Rec ref. In the case of Rec Rec the oxide thickness was 210 to 340 µm while in the Ref Ref case the value is ~ 410 µm, i.e. a more corroded sample in the Ref Ref environment. This agrees with the expectations of the figures **Figure 18** and Figure 19. Only the Ref Rec case exhibits a thin iron oxide, which is suspected to have lost some of the broken iron oxide layers during exposures or sample handing.

The results show that the corrosion memory effect – environment may influence the corrosion rate in two ways. An initially less corrosive deposit may reduce corrosion in a more corrosive environment as it can be observed for the 347H samples in the case of Rec Ref compared to Ref Ref (Figure 18). However, another observation can be made when Ref Rec is compared to Ref Ref: a higher material loss is shown. Therefore, a corrosive deposit may increase the corrosiveness even if it is exposed to a less corrosive environment. The Ref Ref and Rec Rec cases shows that the Sulfur Recirculation has a positive effect on this material even if the material loss is high due to the temperature. However, no corrosion memory could be observed as the values of material loss for Ref Rec and Rec Ref cases are quite close for the low alloyed steel.

6.3 CORROSION MEMORY - MATERIAL

6.3.1 Assessment of corrosion response with respect to microstructure

Previous work has shown that for austenitic steels exposed in biomass boilers, Cr depletion is revealed at the corrosion front and the trend was observed that

increased Cr resulted in more internal attack, especially at high temperatures [14]. In addition, preferential attack especially at grain boundaries was always observed [14, 15, 19, 20]. Other work has observed preferential attack of carbides in chlorine containing atmospheres [11, 21]

From the laboratory experiments with KCl in Section 5.2.1, it is clear that not only the chemical composition affects attack but also the actual microstructure of the steel. The heat treated modified 310 steel shows a five-fold increase of attack compared to the as received steel (not aged microstructure), after only 1 week at 600 °C. This steel was especially chosen because of its high amount of sigma phase (29 vol%) and to reveal the effect of microstructure. Interestingly, the samples revealed quite different internal corrosion morphologies. While the as received sample showed a 'uniform' type of internal corrosion morphology, the heat-treated sample showed a 'selective' type of internal corrosion where interconnecting σ-phase led to deeper attack. Sensitization (due to the precipitation of σ-phase) and / or volatile chromium chloride formation (from the reaction of Cr-rich σ-phase with chlorine) could be reasons for the observed higher, selective type of corrosion attack of the heat-treated sample in KCl bearing environments. As σ-phase is a Cr rich phase, precipitation of σ-phase from the matrix may lead to a Cr depleted zone (sensitization) near to σ-phase. However, the TEM-EDX analysis showed that there was no measurable sensitization near to the σ-phase in the heat-treated sample before corrosion exposure hence, the selective attack and higher corrosion attack in the heat-treated sample in KCl bearing environments cannot be explained based on the mechanism of sensitization. Another mechanism for the observed significantly higher selective internal attack of the heat-treated sample in KCl bearing environments is based on the direct reaction of chromium rich σ-phase with chlorine to easily form Cr-rich volatile chloride followed by formation of oxide through active oxidation [22] and/or ionic transport [23].

For the actual TP347H FG superheater tubes exposed at the power plant for 100,000 hours, sigma phase was also identified at grain boundaries. Compared with the as received steel a similar tendency to that for the modified 310 steel is observed from the laboratory corrosion test, but not to such an alarming extent (Section 5.2.2.) There are very few precipitates for the as-received sample, but for both aged specimens they are present and therefore must be due to the 100,000-hour exposure conditions. Corrosion rates used for lifetime prediction are usually measured on as received steels, and the results indicate that an aged steel has a higher corrosion rate. This could have consequences for converting old boilers to biomass combustion but could also indicate that corrosion rates may increase with ageing, and therefore the thermal history of a component is also relevant.

6.3.2 Microscopy of specimens exposed in the boiler

A comparison of Esshete 1250 in various boiler environments revealed that Cr rich precipitates were clearly present for specimens exposed at high temperatures (Section 5.3.2) where there was grain boundary attack. They were present for both coal-firing and biomass co-firing. At lower temperatures, where there was little grain boundary attack, there was an indication of a darker phase at grain

boundaries, but this was impossible to analyze. At the higher temperatures, the Cr rich precipitates were not present directly at the corrosion front indicating preferential attack and both Cr and Mn sulfides were observed. The actual compositions of these precipitates have not been identified, but their darker colour in the back-scattered image could indicate that they are carbides. The presence of such precipitates on exposed tubes could be due to the following factors:

1. During ageing of steel, the microstructure evolves and precipitates will form at high energy sites such as grain boundaries, similar to the sigma phase observed in the previous section 6.3.1.
2. Where there is a higher temperature, precipitates would be more likely to form through faster kinetics; therefore, there may be increased presence at the fireside since there is a temperature gradient through the wall thickness.
3. If it is carbides, they could form due to the presence of carbon dioxide in the flue gas, and therefore be more prevalent on the flue gas side.
4. Where there is preferential attack of primary or secondary carbides with for example sulfidation or chlorination, then the carbon can be released to form new carbides further into the material.

Since these precipitates are not present at the steam side, this indicates that 3 and 4 are reasons for their presence. The development of sensitized regions from formation of chromium carbides could play a role in both sulfidation (and chlorination). For a nickel based superalloy, grain boundary attack in aged specimens was higher than non-aged in $N_2/H_2/H_2S$ since carbides were preferentially attacked, and where they formed as continuous precipitates there was more attack[24]. For alloy 800 exposed in $H_2/H_2O/H_2S$ environments, carbides were revealed ahead of the sulfides, so carbides reacted at low oxygen partial pressures forming sulfides and releasing carbon further into the material to form more carbides [25]. Thus, the sulfidation reaction results in carbide formation ahead of the corrosion front. Investigation of a gas turbine blade (approx. 700 º C service temperature and 50000 hours exposure) revealed a carbide rich zone below the corrosion front, which indicated inward diffusion of carbon from dissolution of primary carbides as the component oxidizes [26]. A similar mechanism could also be present for Specimen A and B. However, the exact composition of the precipitates is speculation, so further analysis of these precipitates is required with more sophisticated microscopy techniques to understand their role in corrosion. A selective attack of Cr-rich $M_{26}C_6$ and M_3C_7 precipitates has also been reported in chlorine containing environments [11, 21]which could be a reason for the grain boundary attack in biomass environments.

The comparison of different materials in biomass plants reveals internal attack for the austenitic steels, both in biomass only but also in boiler C with biomass and coal fly-ash (Section 5.3.2). Comparison of etched TP347H components from the penthouse and within the boiler reveals a different susceptibility to etching at the fireside for specimens in the flue gas stream which indicates increased precipitation or sensitisation. SEM analysis of 18% Cr austenitic steels identifies dark precipitates similar to those observed in Section 5.3, but they are only sporadically present. Since

a broad band of precipitates was present for TP347H exposed for 100000 hours in boiler C, this was investigated with TEM, and Cr rich $M_{23}C_6$ were detected at the grain boundary. This could give the indication that similar Cr rich $M_{23}C_6$ precipitates may be present on the fireside of specimens from boilers where biomass only had been present, as they have a similar appearance in the SEM-BSE image, however further analyses is required to confirm this hypothesis.

7 Conclusions

- The full-scale Sulfur Recirculation technique installed in the CHP plant MEC changes the deposit chemistry and less corrosive species end up on the superheaters. This results in less corrosion of the superheaters both on low alloyed steals and on stainless steels, which will increase the superheater life time and decrease the cost for replacements. Alternatively, the steam data and electricity production may be increased in this plant and also in new plants using Sulfur Recirculation.
- The first commercial full scale Sulfur Recirculation installation at MEC has in this work provided an excellent platform in order to study the environmental corrosion memory effect with the two parallel lines representing different corrosive fuels.
- The results show that the corrosion memory effect – environment may influence the corrosion rate in two ways. An initially less corrosive deposit may reduce corrosion in a more corrosive environment while a corrosive deposit may increase corrosion in a less corrosive environment.
- From laboratory experiments, steels of the same composition behaved differently due to the presence of Cr rich precipitates. The preferential attack of Cr rich sigma phase in KCl bearing environments has been shown for the modified heat treated 310 steel, compared to the as received. In addition, aged 347H FG from a power plant had a faster corrosion rate than the as received steel. This knowledge may be used to improve material selection of superheaters or identify possible risks for corrosion when changing temperature/environment.
- Cr rich precipitates were revealed at the corrosion front for lean austenitic steels exposed in the plant in different combustion environments, i.e. coal, clean wood pellets + oil, clean wood pellets + coal-fly ash. These Cr rich precipitates were identified in one case to be $M_{23}C_6$.

8 Goal fulfilment

8.1 PROJECT GOALS

The overall goal of the project was to investigate strategies to improve plant economy and to increase the green electricity production. This has been achieved through research in a full-scale installation of a novel corrosion mitigation technique called Sulfur Recirculation as well as demonstrating the corrosion memory effect.

The project aim was to show how the corrosion attack of the superheaters is altered when the Sulfur Recirculation technique is activated. The aim was in addition to generate new knowledge of two aspects of corrosion memory. These tasks have been carried out successfully and the project knowledge may lead to improved plant economy by:

- Increased fuel flexibility
- Increased steam data
- Better material selection in order to improved long term corrosion resistance

Furthermore, the project has deployed a unique approach in corrosion testing. In order to investigate the long-term behaviour of selected superheater materials, well-controlled pre- treatments were performed to samples prior to the exposures. Thus, linking environment to the development of the different alloys gave a unique possibility to predict the long-time behaviour in different types of environment.

8.2 KME GOALS

This project has directly worked towards fulfilling the following KME Goals:

KME Goal 1: *To examine opportunities and obstacles with regard to how plants in Sweden can achieve greater steam data corresponding to the long-term ambition of electrical efficiency that is 3-4 percentage units higher than the best technology for a given fuel at present.*

This project has examined how the corrosion attack is changed when the Sulfur Recirculation technique was deployed. This knowledge/data showed that the electrical efficiency could be increased with maintained corrosion rates. Higher steam data and higher electrical efficiency from biogenic fuels is the ultimate goal of this project. It was anticipated that the sulfur technique would lead to a decrease in deposit formation, resulting in a higher heat transfer of the superheater tubes. The expected deposit rate decrease has not been observed during these tests.

KME Goal 2: *To further develop tools and techniques to facilitate the application of new material solutions in plants.*

The obtained generic knowledge about the long-term material behaviour may aid the material manufacturers in producing steels with optimized microstructural properties

KME Goal 3: *To evaluate exposures and application tests of various solid and composite materials and/or coated materials with the aim to develop improved material solutions which help to bring about greater fuel flexibility and increased electricity production.*

This project has examined how already aged materials perform in an environment that mimic biomass and waste combustion. The aged materials included materials with different precipitate distributions. The results will assist in an improved material selection of optimum superheater materials for prolonged lifetime and may aid material manufacturers in producing steels with optimized microstructural properties.

KME Goal 5: *Suggestions for measures and solutions in order to reduce superheater and furnace corrosion, erosion-related problems and low temperature corrosion should have been developed.*

This project examined how successful the corrosion mitigation technique "Sulfur Recirculation" was for decreasing corrosion of superheaters in a waste fired boiler.

KME Goal 6: *Suggestions for new design solutions, operating parameters and tools for assessing what technical demands a specific fuel places on the plant should have been developed for CHP plants with the aim to help achieve enhanced fuel flexibility and availability.*

This project examined how the corrosion mitigation technique "Sulfur Recirculation" affected the flue gas chemistry of a waste fired boiler (primarily with respect to SO_2), and thus, the fuel flexibility and/or the availability can be increased. Furthermore, by an improved knowledge of how the corrosion attack is affected over time (not only the initial attack) by environmental- and material specific parameters new design solutions, operating parameters and tools can be suggested.

KME Goal 9: *To develop methods for quantifying process ability for new materials, as well as creating an understanding of microstructure development and mechanical properties for more efficient energy plants.*

The obtained generic knowledge about the long-term material behaviour may aid the material manufacturers in producing steels with optimized microstructural properties

9 Suggestions for future research work

This project has investigated the first full scale installation of the Sulfur Recirculation technique during a limited time. The results are very promising but in order to better understand the long-term impact and the full potential longer exposures would be interesting to investigate.

In the project several aspects of the corrosion memory effect have been investigated. The results have enlightened various aspects and possibilities. However, the results obtained within the project have also raised many suggestions for further studies. Especially, if the questions addressed in the project should be scientifically answered a more extensive exposure matrix needs to be performed, investigating the different steps more thoroughly. It would in addition be interesting to increase the temperature range as the positions limited the highest temperature in this case.

Taking in account the results obtained in the project and the analysis presented above, some further studies could be proposed to improve the knowledge about the dynamic corrosion and memory effect, which has started in this project. The two different memory effects could in addition be combined in a future investigation. Would an aged material be more vulnerable to a change of fuel?

10 Literature references

[1] S. Andersson, E. W. Blomqvist, L. Bafver, F. Jones, K. Davidsson, J. Froitzheim, M. Karlsson, E. Larsson and J. Liske. 2014. Sulfur Recirculation for increased electricity production in Waste-to-Energy plants. Waste Management, 34, 67-78.
[2] H. Hunsinger, H. Seifert and K. Jay. 2007. Reduction of PCDD/F formation in MSWI by a process-integrated SO_2 cycle. Environmental Engineering Science, 24, 1145-1159.
[3] H. Hunsinger and S. Andersson. 2014. The potential of SO_2 for reducing corrosion in WtE plants. Journal of Material Cycles and Waste Management, 16, 657-664.
[4] P. Henderson, P. Szakálos, R. Pettersson, C. Andersson and J. Högberg. 2006. Reducing superheater corrosion in wood-fired boilers. Materials and Corrosion, 57, 128-134.
[5] S. Karlsson, J. Pettersson, J. E. Svensson and L. G. Johansson. 2011. KCl-Induced high temperature corrosion of the austenitic stainless steel 304L - The influence of SO_2. 696, 224-229.
[6] H. Kassman, J. Pettersson, B. M. Steenari and L. E. Åmand. 2013. Two strategies to reduce gaseous KCl and chlorine in deposits during biomass combustion - Injection of ammonium sulphate and co-combustion with peat. Fuel Processing Technology, 105, 170-180.
[7] H. H. Krause, D. A. Vaughan and W. K. Boyd. 1975. Corrosion and Deposits from Combustion of Solid-Waste .3. Effects of Sulfur on Boiler Tube Metals. Journal of Engineering for Power-Transactions of the Asme, 97, 448-452.
[8] J. Pettersson, N. Folkeson, L. G. Johansson and J. E. Svensson. 2011. The effects of KCl, K $2SO_4$ and K_2CO_3 on the high temperature corrosion of a 304-type austenitic stainless steel. Oxidation of Metals, 76, 93-109.
[9] E. Vainio, P. Yrjas, M. Zevenhoven, A. Brink, T. Laurén, M. Hupa, T. Kajolinna and H. Vesala. 2013. The fate of chlorine, sulfur, and potassium during co-combustion of bark, sludge, and solid recovered fuel in an industrial scale BFB boiler. Fuel Processing Technology, 105, 59-68.
[10] P. Viklund, R. Pettersson, A. Hjörnhede, P. Henderson and P. Sjövall. 2009. Effect of sulphur containing additive on initial corrosion of superheater tubes in waste fired boiler. Corrosion Engineering Science and Technology, 44, 234-240.
[11] H. Fujikawa and N. Maruyama. 1989. Corrosion Behavior of Austenitic Stainless-Steels in the High Chloride-Containing Environment. Materials Science and Engineering a-Structural Materials Properties Microstructure and Processing, 120, 301-306.
[12] O. H. Larsen and M. Montgomery. 2006. Materials problems and solutions in biomass fired plant. Energy Materials: Materials Science and Engineering for Energy Systems, 1, 227-237.
[13] M. Montgomery, S. A. Jensen, U. Borg, O. Biede and T. Vilhelmsen. 2011. Experiences with high temperature corrosion at straw-firing power plants in Denmark. Materials and Corrosion, 62, 593-605.
[14] M. Montgomery and A. Karlsson. 1999. In-situ corrosion investigation at Masnedo CHP plant - a straw-fired power plant. Materials and Corrosion-Werkstoffe Und Korrosion, 50, 579-584.
[15] M. Montgomery, A. Karlsson and O. H. Larsen. 2002. Field test corrosion experiments in Denmark with biomass fuels Part 1: Straw-firing. Materials and Corrosion-Werkstoffe Und Korrosion, 53, 121-131.
[16] L. Korcakova and e. al. 2013. Investigations of superheater materials from Nordjyllandsværket coal-fired plant after 100000 hours service.
[17] S. Kiamehr, K. V. Dahl, M. Montgomery and M. A. J. Somers. 2016. KCl-induced high temperature corrosion of selected commercial alloys Part II: alumina and silica-formers. Materials and Corrosion-Werkstoffe Und Korrosion, 67, 26-38.
[18] T. Jonsson, A. Järdnäs, J. E. Svensson, L. G. Johansson and M. Halvarsson. 2007. The effect of traces of SO_2 on iron oxidation: A microstructural study. Oxidation of Metals, 67, 193-213.

[19] C. Liu, J. A. Little, P. J. Henderson and P. Ljung. 2001. Corrosion of TP347H FG stainless steel in a biomass fired PF utility boiler. Journal of Materials Science, 36, 1015-1026.
[20] M. Montgomery and e. al. 2010.
[21] H. J. Grabke, M. Spiegel and A. Zahs. 2004. Role of alloying elements and carbides in the chlorine-induced corrosion of steels and alloys. Materials research 7, 89-95.
[22] H. J. Grabke, E. Reese and M. Spiegel. 1995. The effects of chlorides, hydrogen chloride, and sulfur dioxide in the oxidation of steels below deposits. Corrosion Science, 37, 1023-1043.
[23] N. Folkeson, T. Jonsson, M. Halvarsson, L. G. Johansson and J. E. Svensson. 2011. The influence of small amounts of KCl(s) on the high temperature corrosion of a Fe-2.25Cr-1Mo steel at 400 and 500°C. Materials and Corrosion, 62, 606-615.
[24] H. Yakuwa, M. Miyasaka, S. Nakahama, T. Ohno, T. Uehara, T. Nonomura and T. Narita. 2002. Effect of titanium and aluminum contents on the grain-boundary sulfidation of a nickel-based superalloy. Corrosion, 58, 646-658.
[25] D. S. Williams, R. Moller and H. J. Grabke. 1981. The High-Temperature Corrosion of Alloy-800 in Carburizing, Oxidizing, and Sulfidizing Environments. Oxidation of Metals, 16, 253-266.
[26] K. V. Dahl and J. Hald. 2013. Identification of Precipitates in an IN792 Gas Turbine Blade after Service Exposure. Praktische Metallographie-Practical Metallography, 50, 432-450.

11 Publications

- Y.C. Malede, M. Montgomery, K.V. Dahl J. Hald: "Effect of microstructure on KCl corrosion attack of modified AISI 310 steel Materials at High Temperatures" Vol 35, No 1-3, 2018 pp243-254.
- K.V. Dahl, A. Slomian, T.N. Lomholt, S. Kiamehr, F.B. Grumsen, M. Montgomery, T. Jonsson: "Characterization of pack cemented Ni2Al3 coating exposed to KCl(s) induced corrosion at 600ºC, Materials at High Temperatures", Vols 35, No1-3, pp 267-274.
- M. Montgomery, K.V. Dahl, S.A. Jensen, C. Davies: "High Temperature Fireside Corrosion of Esshete 1250 in Coal, Co-firing with Biomass and Biomass Power Plants". Proceedings Eurocorr 2017, Prague 3-7th September, 2017.
- Y.C. Malede, K.V. Dahl, M. Montgomery, J. Hald: "Effect of ageing on KCl corrosion attack of AISI 347H FG steel". Proceedings Eurocorr 2017, Prague 3-7th September, 2017
- S. Andersson, M.D. Paz, J. Phother, T. Jonsson: "High Temperature Corrosion and Dioxin Abatement using Sulfur Recirculation in a Waste-to-Energy Plant" accepted for Oral presentation at 7th international symposium on energy from biomass and waste, Venice, 15-18 October 2018.
- M.D. Paz, J. Phother, S. Andersson, T. Jonsson: "Sulfur Recirculation as a tool for high temperature corrosion abatement." Accepted for Impacts of Fuel Quality in Power Production and the Environment, Lake Louise, AB, Canada 24-28th September 2018
- M.D. Paz, J. Phother, S. Andersson, T. Jonsson. "Influence of the Sulfur Recirculation boiler operation on the future corrosion rate". Accepted for Impacts of Fuel Quality in Power Production and the Environment, Lake Louise, AB, Canada 24-28th September 2018

Sulfur recirculation and improved material selection for high temperature corrosion abatement

This project has investigated strategies to improve plant economy and to increase electricity production from waste and biomass.

Sulfur Recirculation has been shown to decrease the high temperature corrosion rates of superheaters in a full-scale installation, which may increase green electricity production from combustion of biomass and waste in the future. Furthermore, the project results have demonstrated the corrosion memory effect. The gained insights in the corrosion memory effects may be used to optimize operation to increase superheater life time, thereby decrease the environmental impact from exchanging superheater steel tubes.

This knowledge may lead to improved plant economy by:

- Increased fuel flexibility
- Increased steam data
- Better material selection in order to improved long term corrosion resistance

Furthermore, the project has deployed a unique approach in corrosion testing. In order to investigate the long-term behaviour of selected superheater materials, well-controlled pre- treatments were performed to samples prior to the exposures. Thus, linking environment to the development of the different alloys gave a unique possibility to predict the long-time behaviour in different types of environment.